Supporting Information

Controlling the Kinetics of Self-Reproducing Micelles by Catalyst Compartmentalization in a Biphasic System

Elias A. J. Post and Stephen P. Fletcher*

Department of Chemistry, Chemistry Research Laboratory, University of Oxford, 12 Mansfield Road, Oxford, OX1 3TA, U.K.

Corresponding Author: stephen.fletcher@chem.ox.ac.uk

TABLE OF CONTENTS **S1**

NMR SPECTRA OF SYNTHESIZED COMPOUNDS

^{1}H NMR spectrum of **3** S3
^{13}C NMR spectrum of **3** S3
^{1}H NMR spectrum of **13** S4
^{13}C NMR spectrum of **13** S4
^{1}H NMR spectrum of **17** S5
^{13}C NMR spectrum of **17** S5
^{1}H NMR spectrum of **18** S6
^{13}C NMR spectrum of **18** S6
^{1}H NMR spectrum of **4** S7
^{13}C NMR spectrum of **4** S7
^{1}H NMR spectrum of **19** S8
^{13}C NMR spectrum of **19** S8
^{1}H NMR spectrum of **6** S9
^{13}C NMR spectrum of **6** S9
^{1}H NMR spectrum of **7** S10
^{13}C NMR spectrum of **7** S10
^{31}P NMR spectrum of **7** S11
^{1}H NMR spectrum of **8** S11
^{13}C NMR spectrum of **8** S12
^{31}P NMR spectrum of **8** S12

DOSY DATA **S13**

FLUORIMETRY DATA **S14**

DLS DATA **S16**

KINETIC DATA **S18**

^{1}H NMR spectra of key water soluble reaction components in D_2O S18
Stacked Spectra of Kinetic ^{1}H NMR Experiments S21

Tables of extracted reaction rates S27
Control experiments S28

REFERENCES **S30**

NMR Spectra of Synthesized Compounds

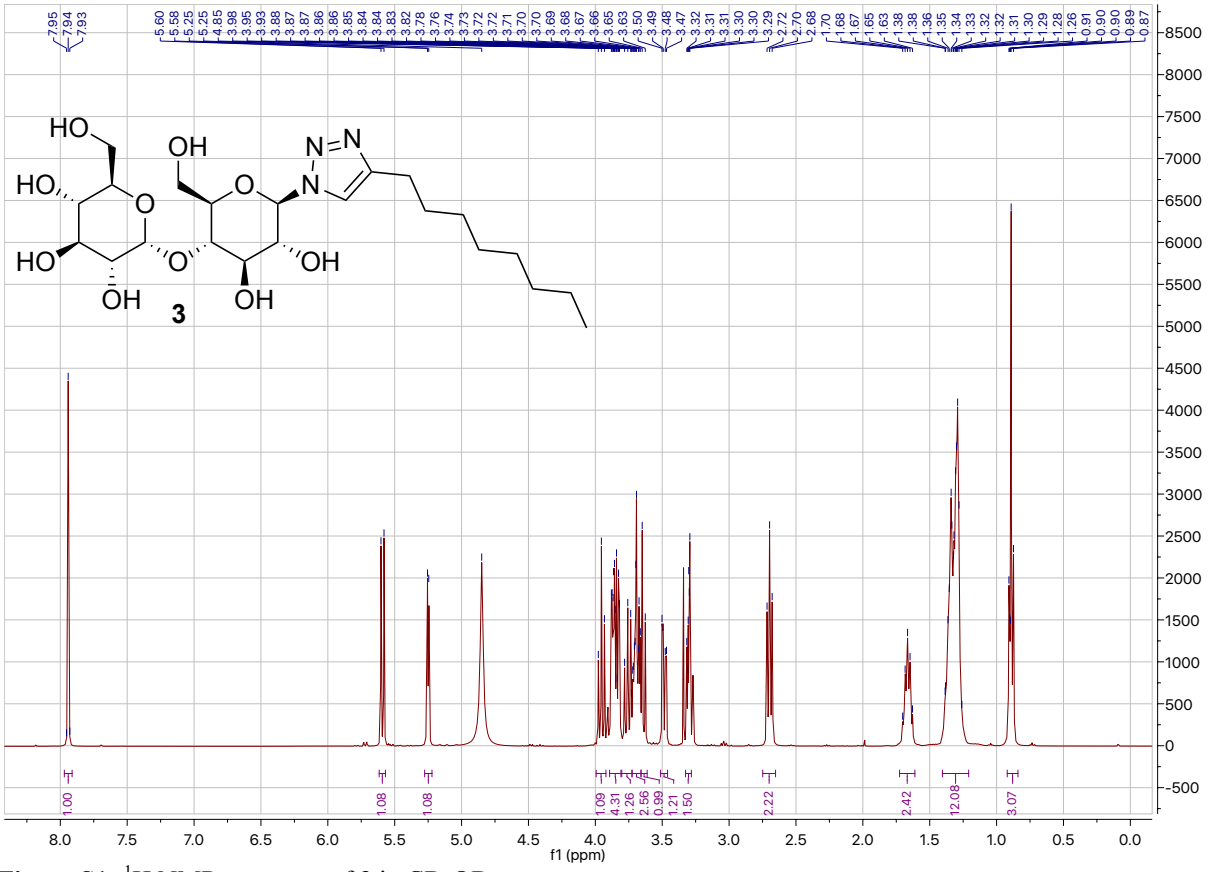

Figure S1: ^{1}H NMR spectrum of **3** in CD_3OD.

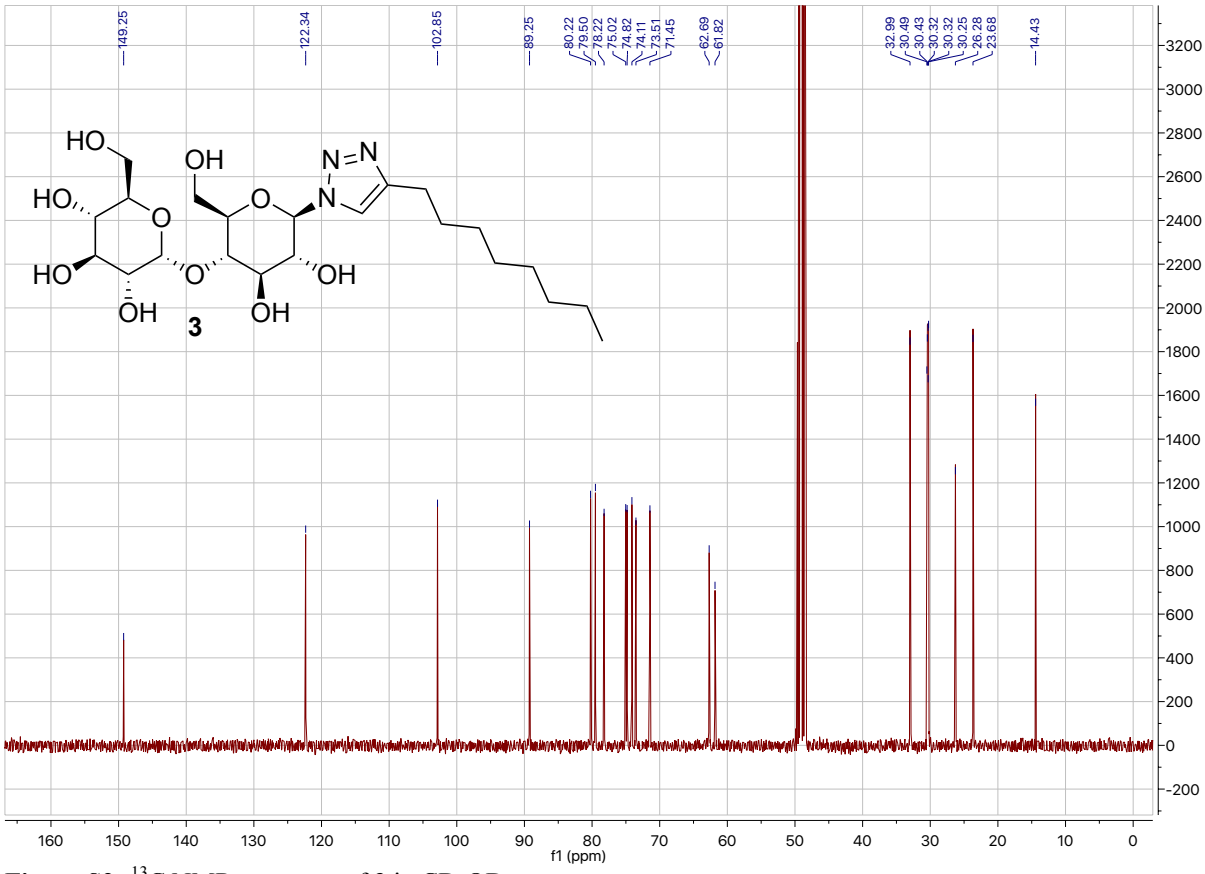

Figure S2: ^{13}C NMR spectrum of **3** in CD_3OD.

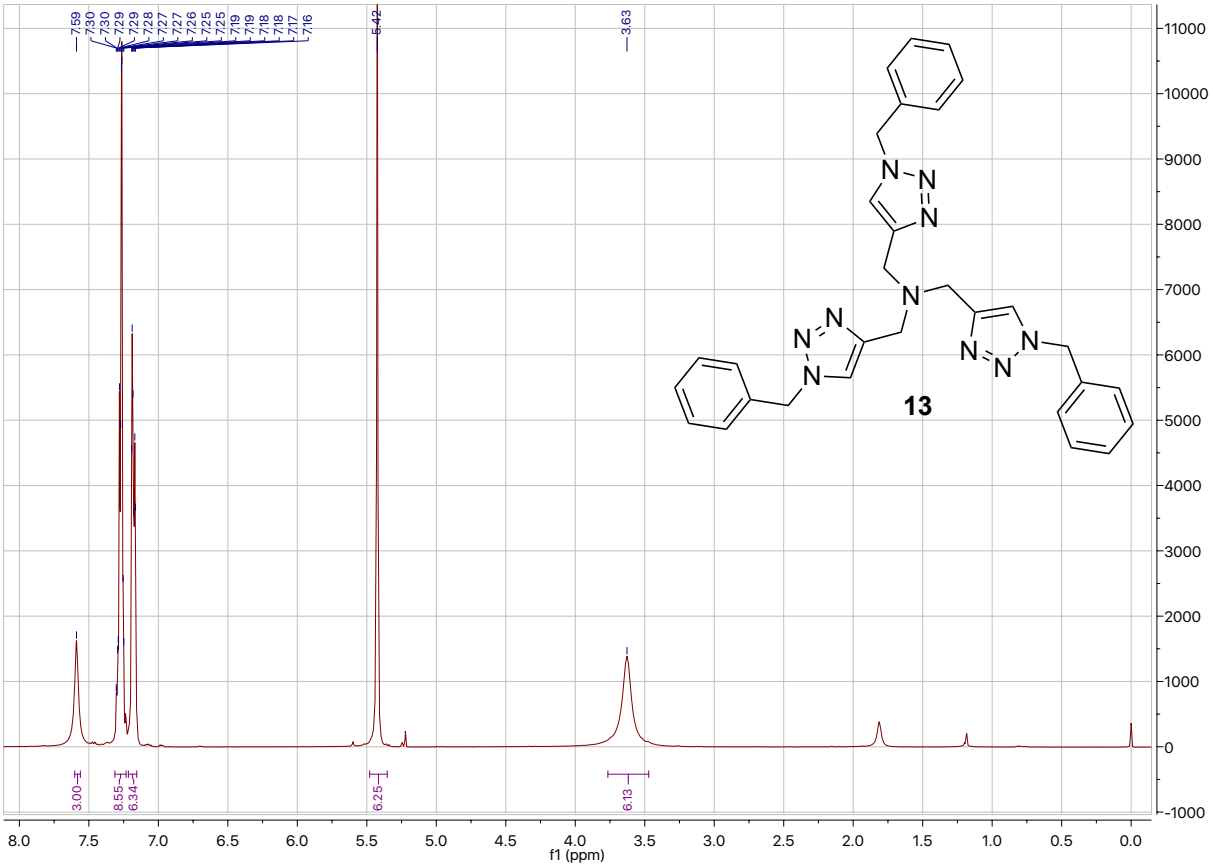

Figure S3: ^{1}H NMR spectrum of **13** in $CDCl_3$.

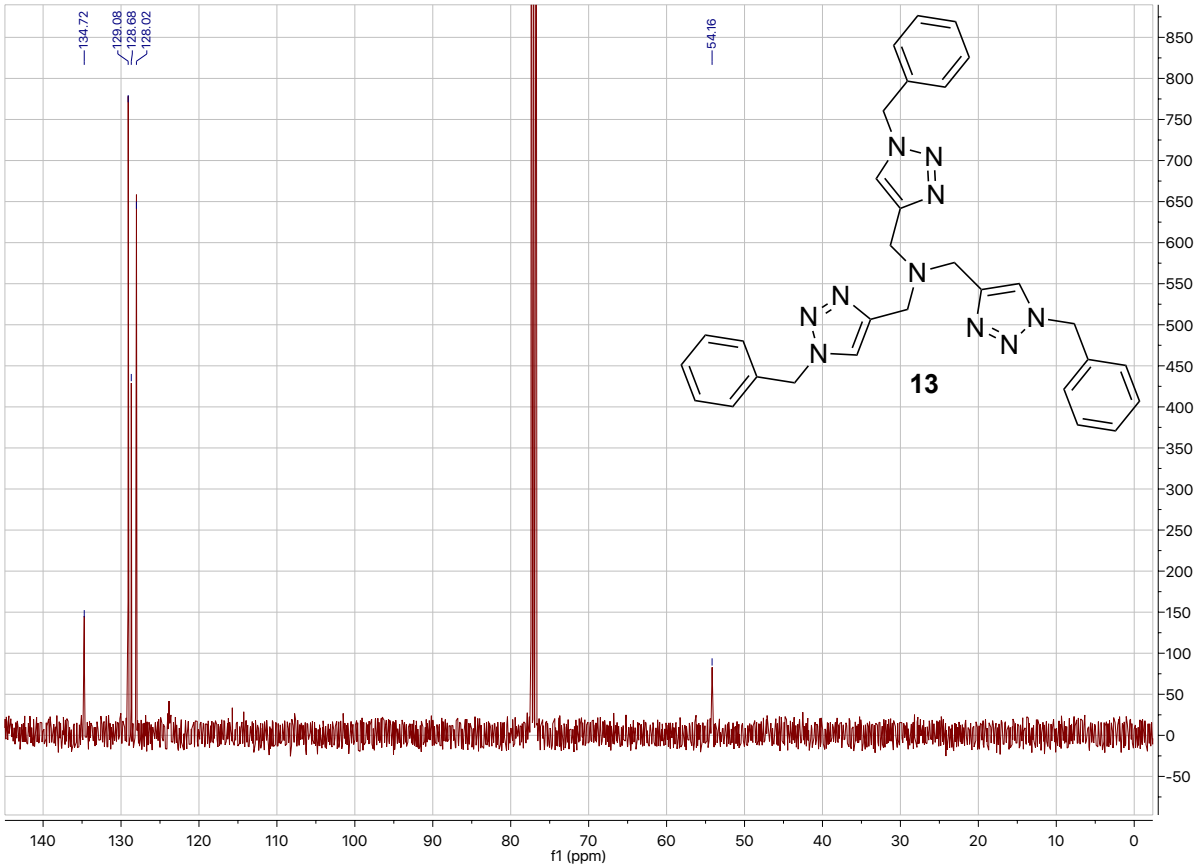

Figure S4: ^{13}C NMR spectrum of **13** in $CDCl_3$.

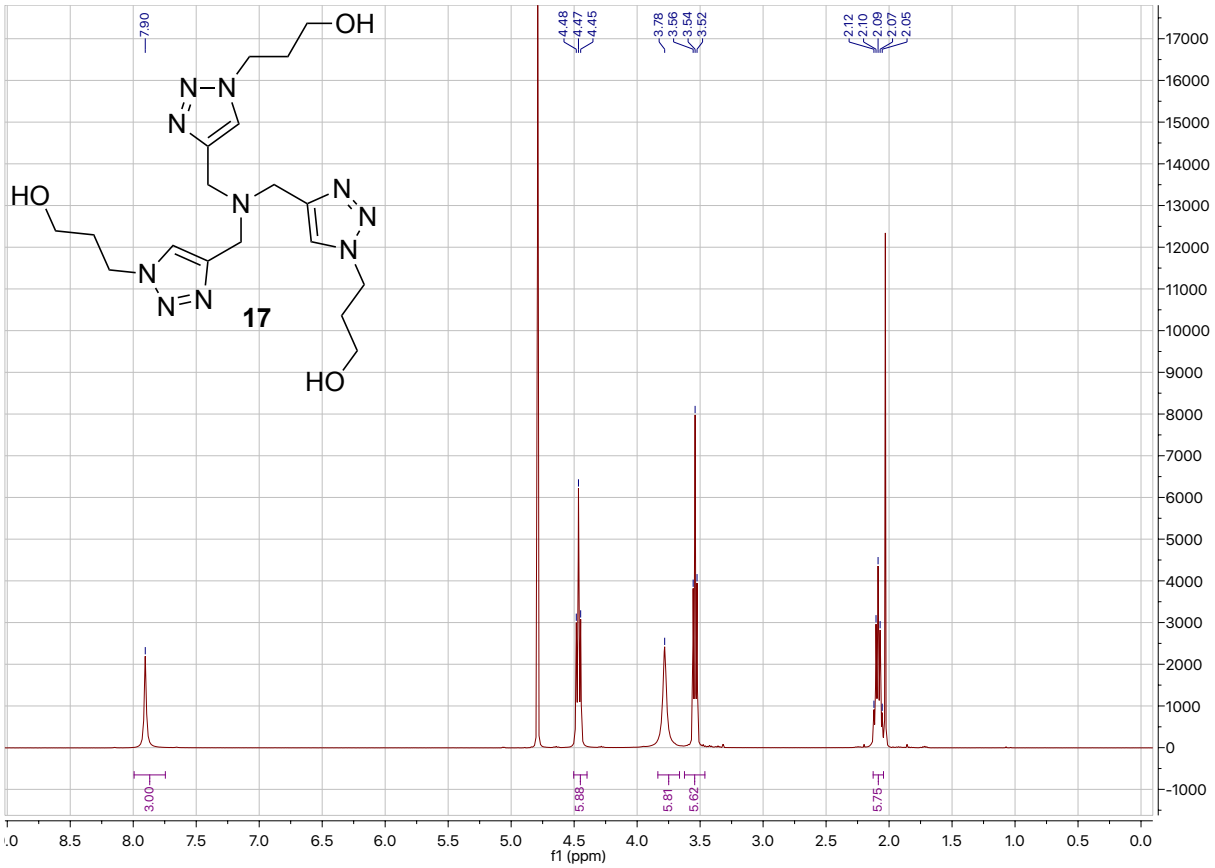

Figure S5: ^{1}H NMR spectrum of **17** in D_2O.

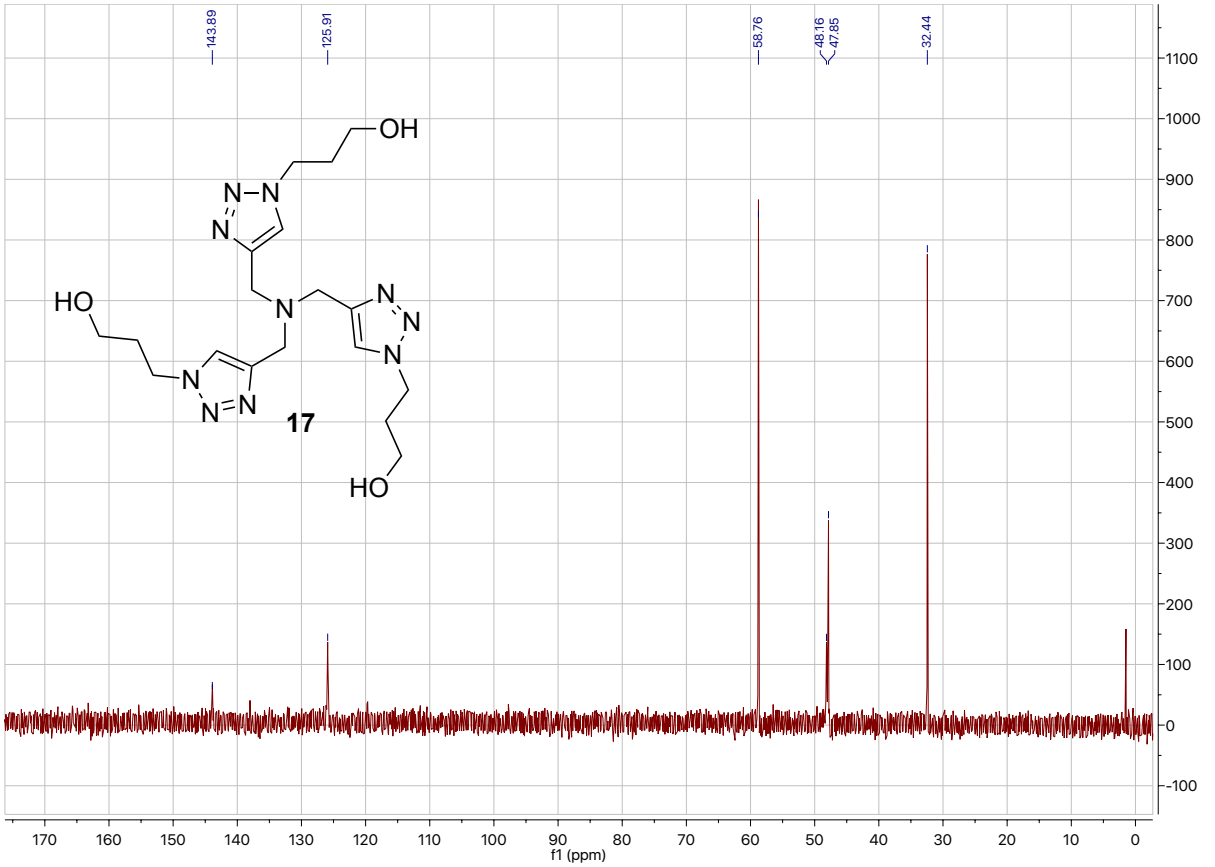

Figure S6: ^{13}C NMR spectrum of **17** in D_2O.

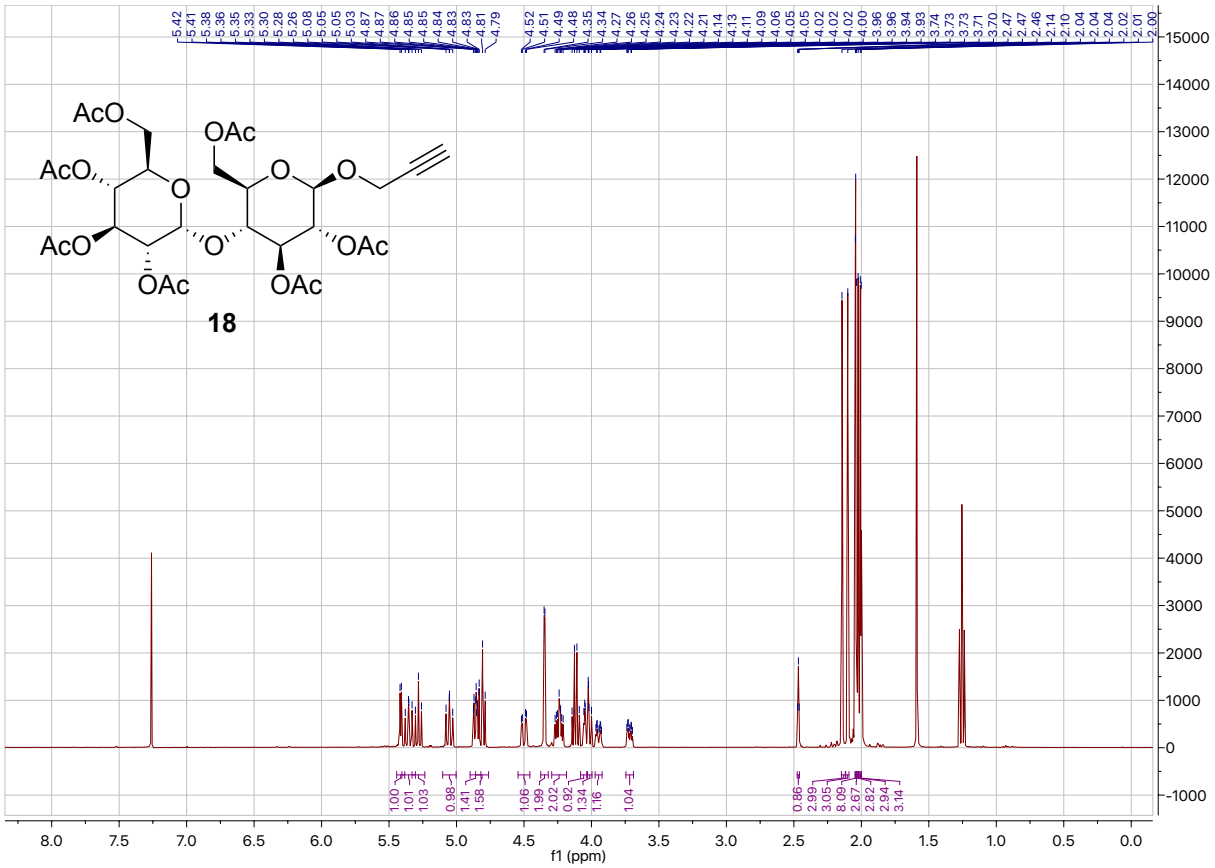

Figure S7: ^{1}H NMR spectrum of **18** in $CDCl_3$.

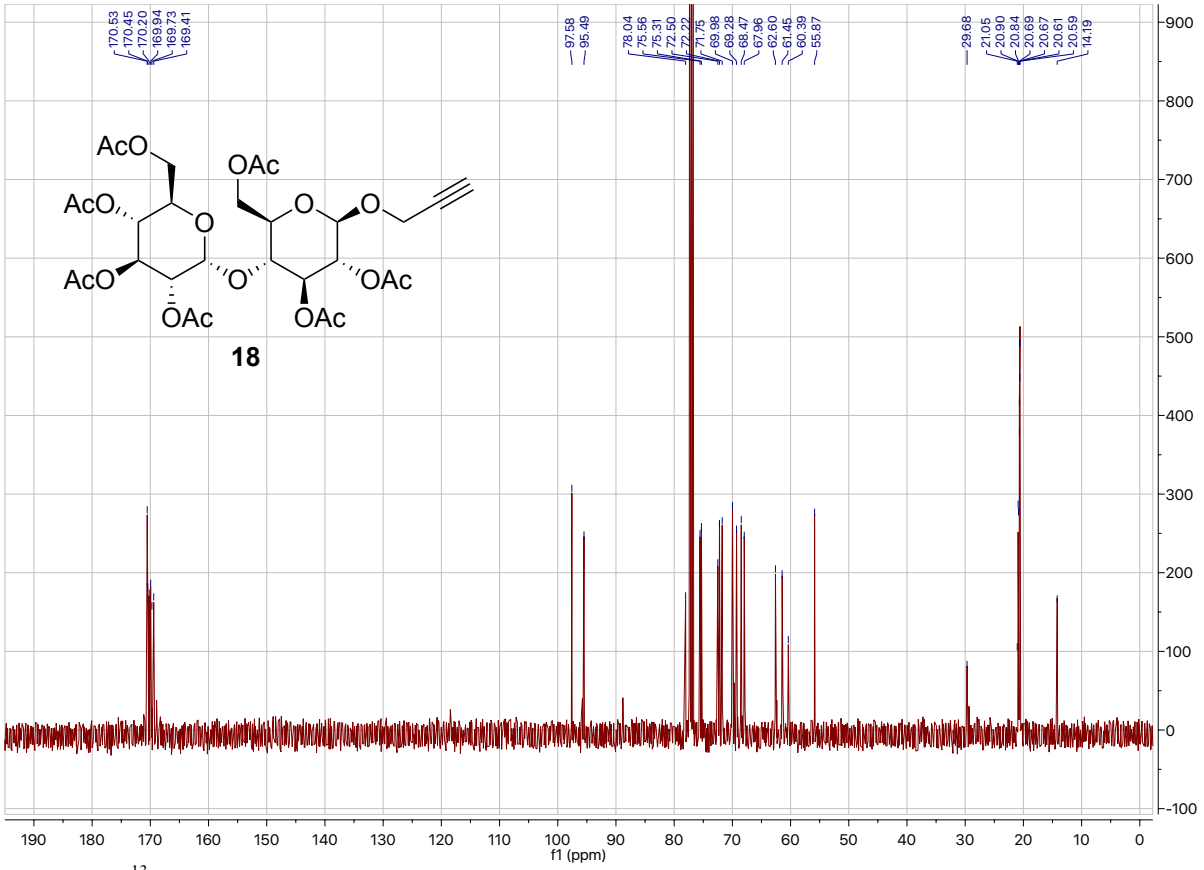

Figure S8: ^{13}C NMR spectrum of **18** in $CDCl_3$.

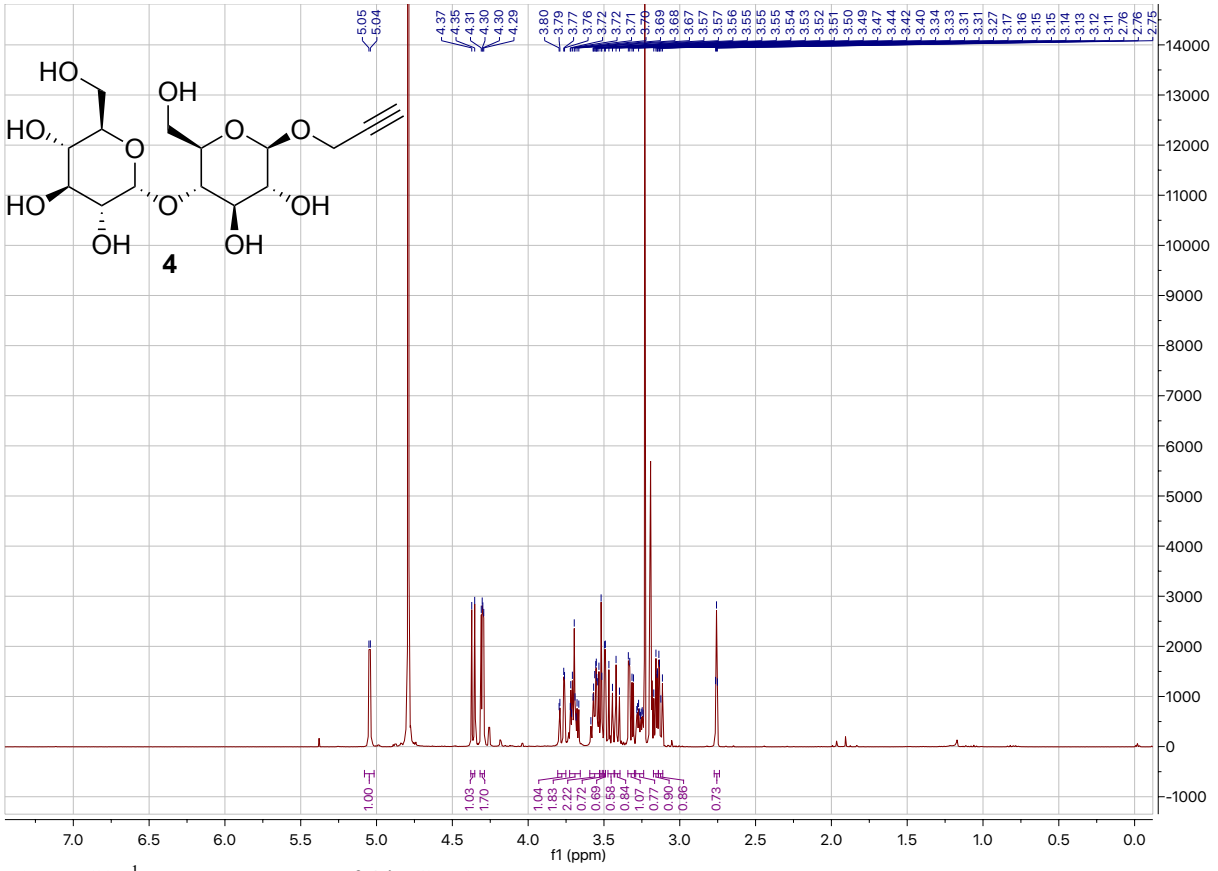

Figure S9: ^{1}H NMR spectrum of **4** in CD_3OD.

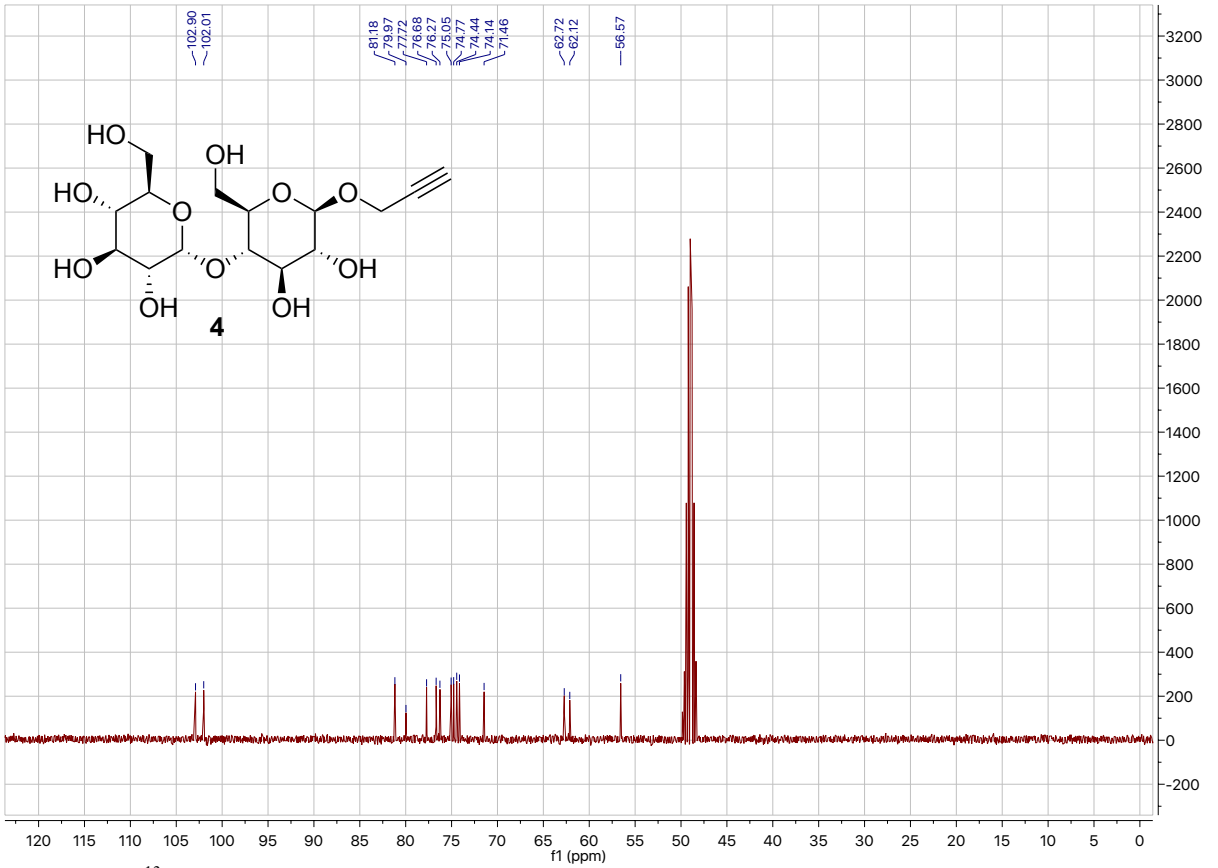

Figure S10: ^{13}C NMR spectrum of **4** in CD_3OD.

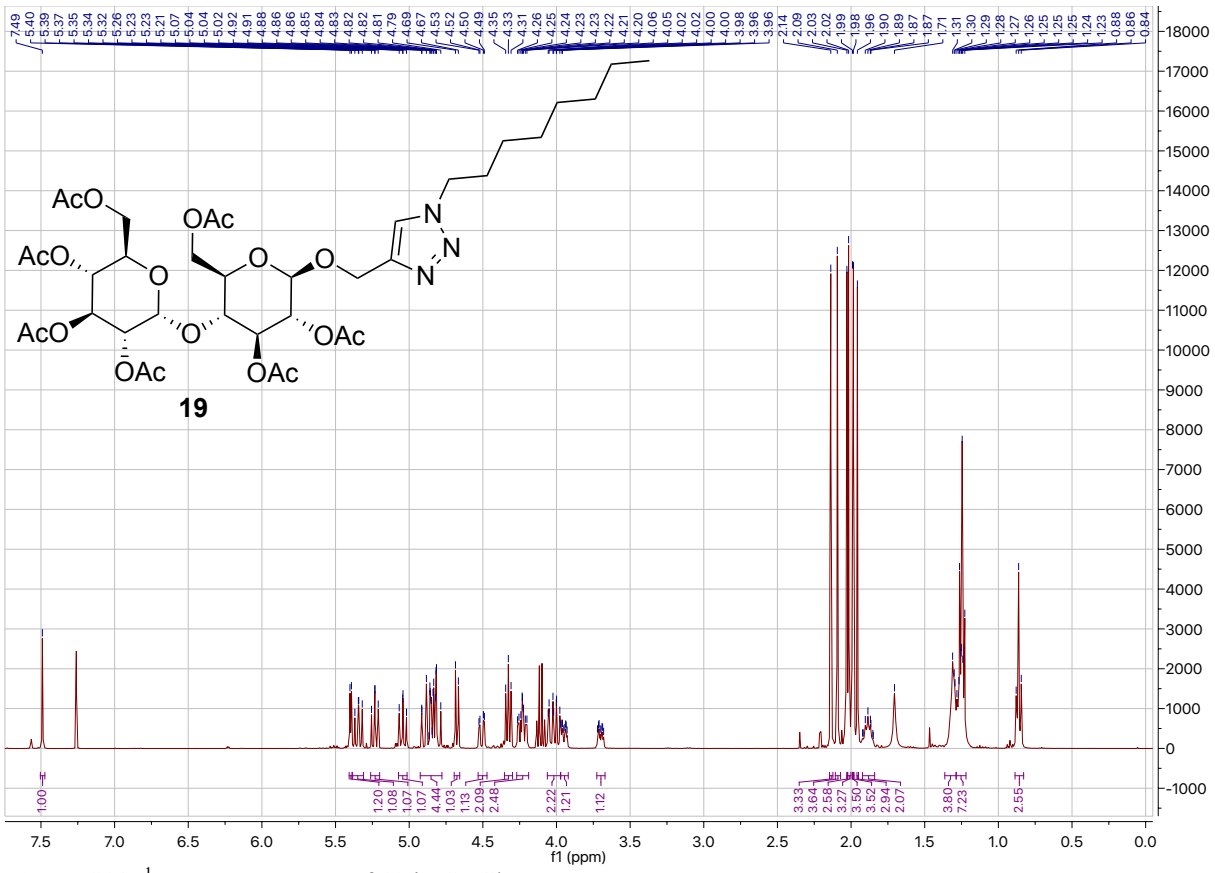

Figure S11: ^{1}H NMR spectrum of **19** in $CDCl_3$.

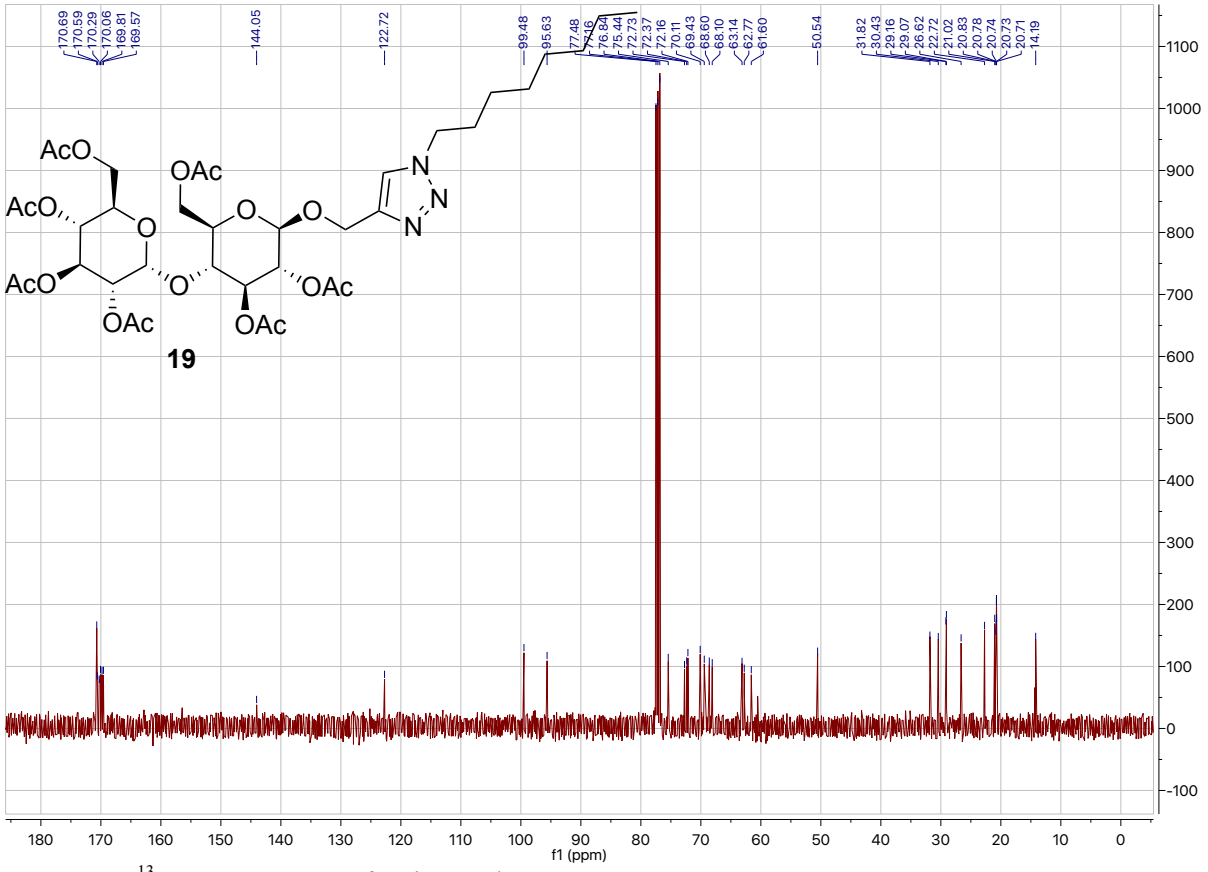

Figure S12: ^{13}C NMR spectrum of **19** in $CDCl_3$.

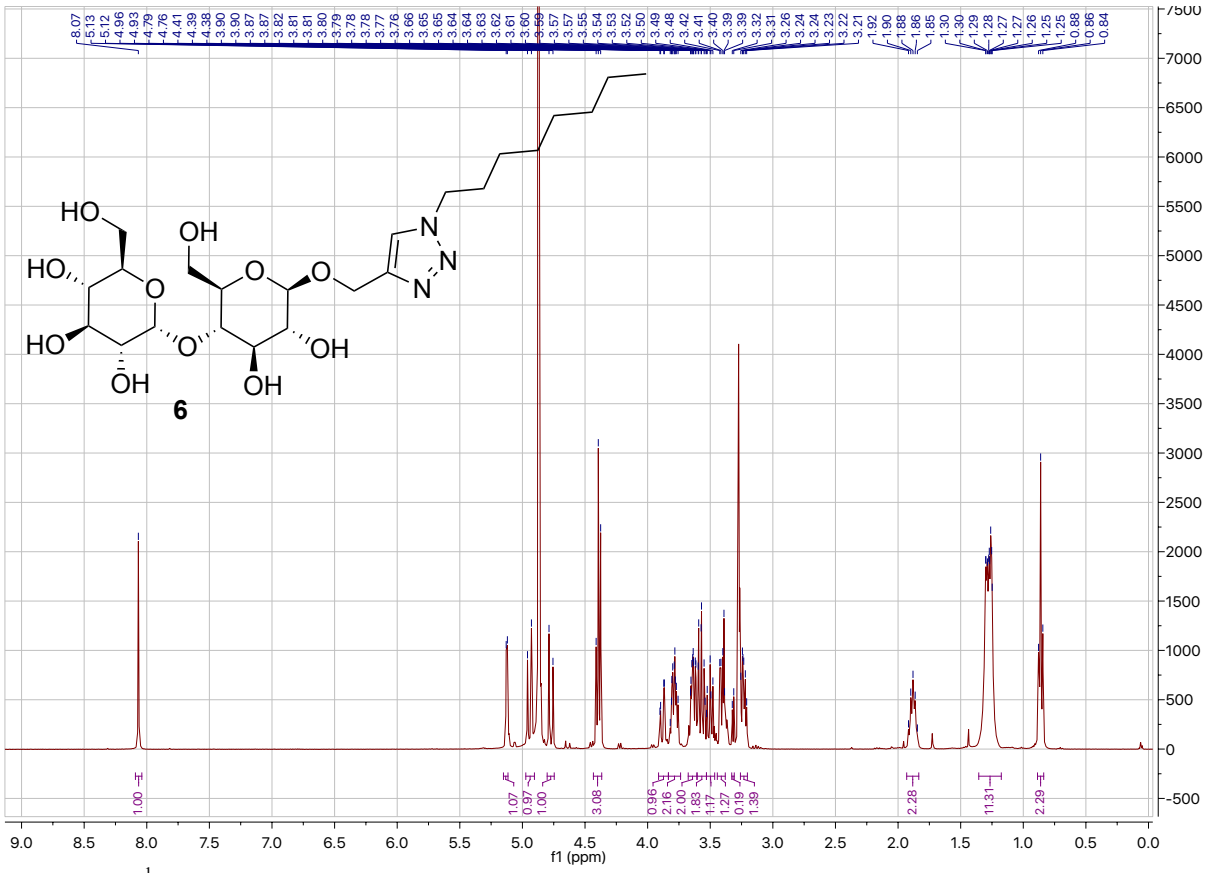

Figure S13: ^{1}H NMR spectrum of **6** in CD_3OD.

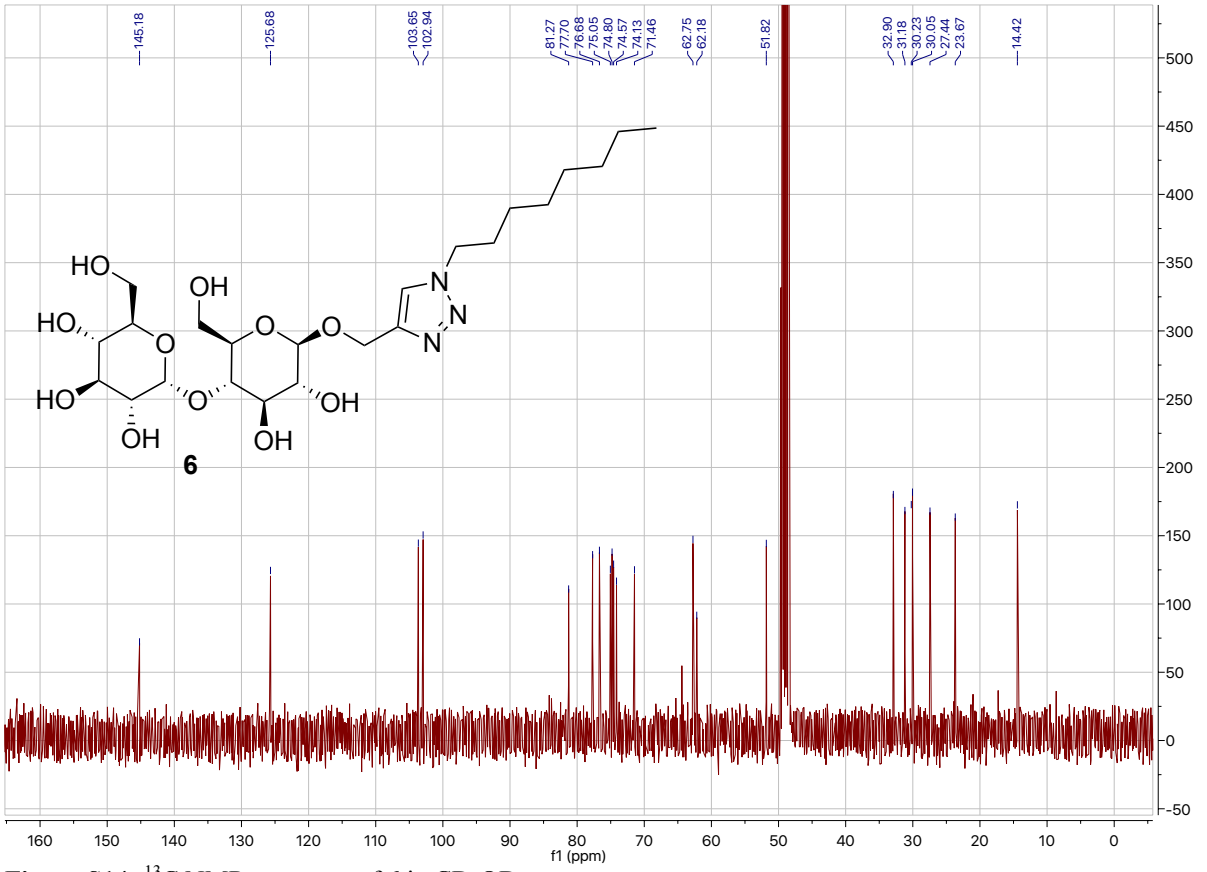

Figure S14: ^{13}C NMR spectrum of **6** in CD_3OD.

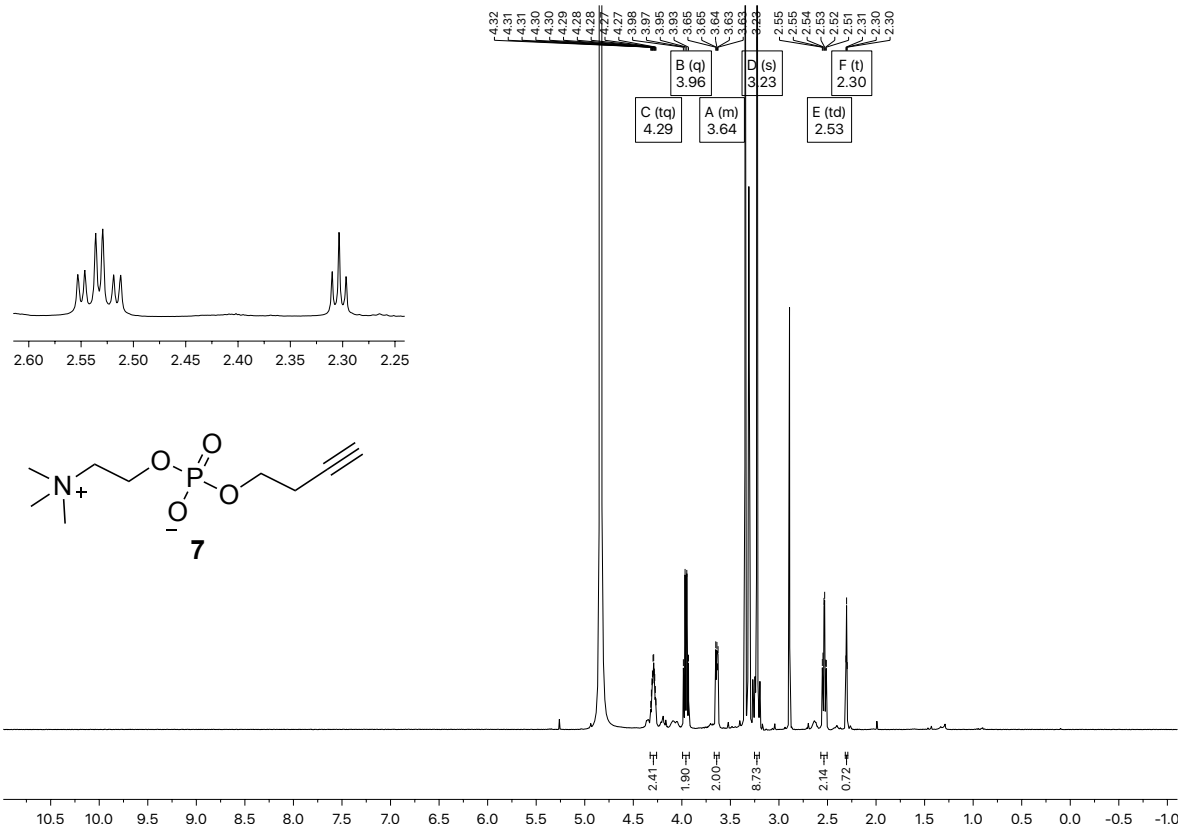

Figure S15: ^{1}H NMR spectrum of **7** in CD_3OD.

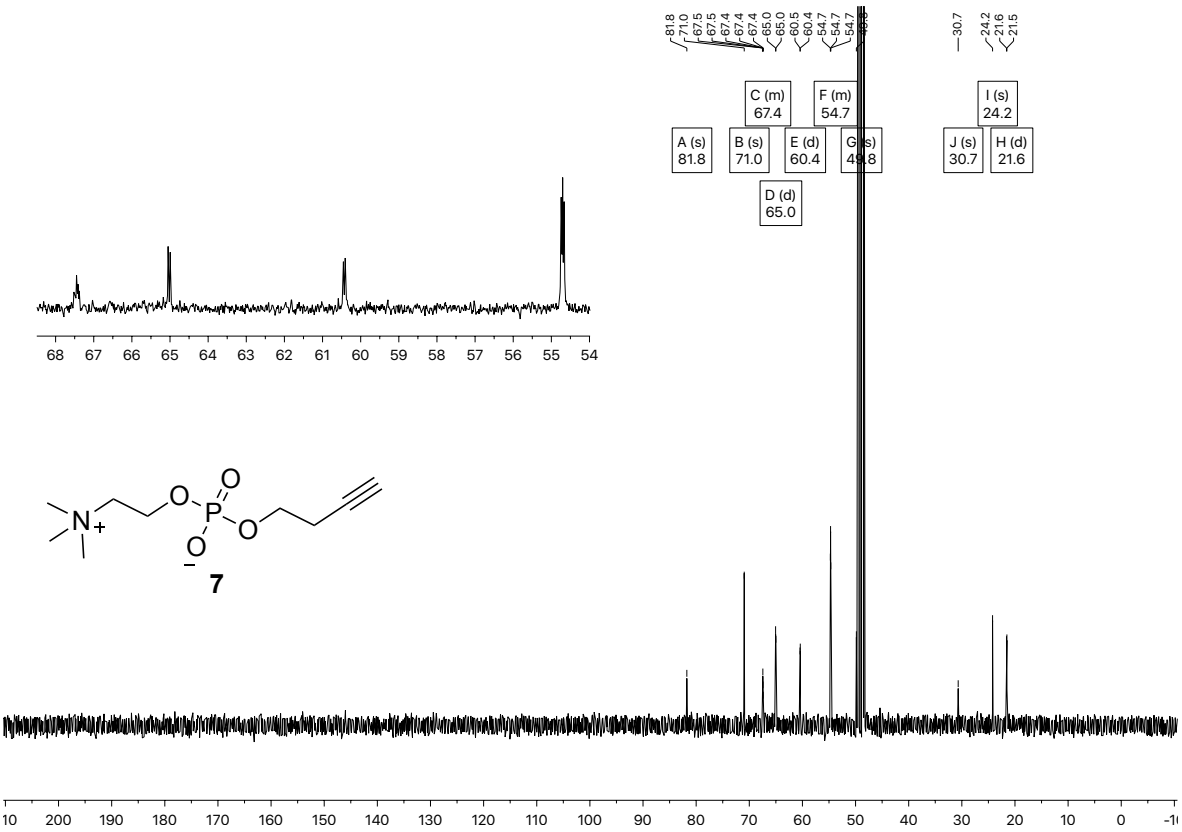

Figure S16: ^{13}C NMR spectrum of **7** in CD_3OD.

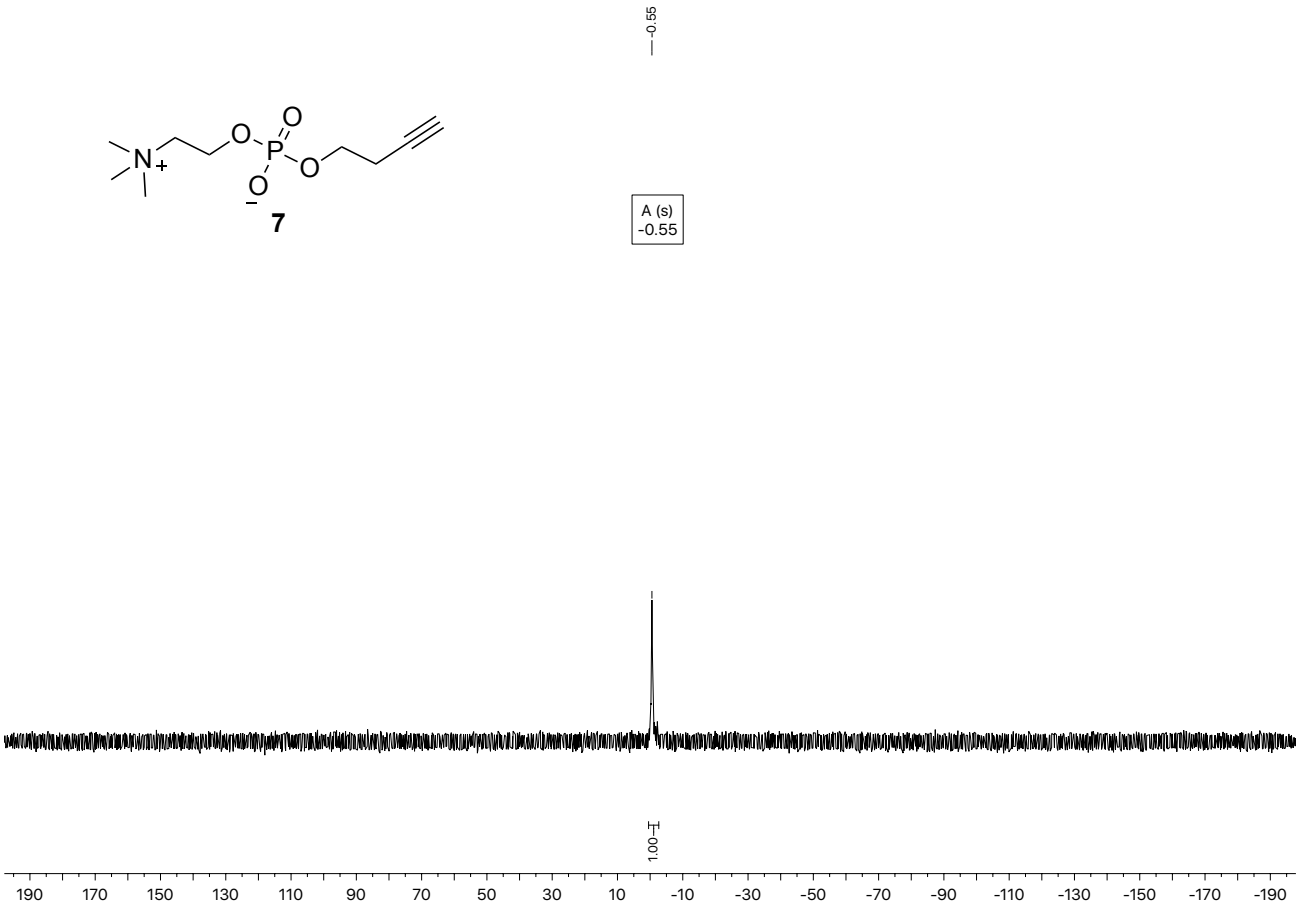

Figure S17: ^{31}P NMR spectrum of **7** in CD_3OD.

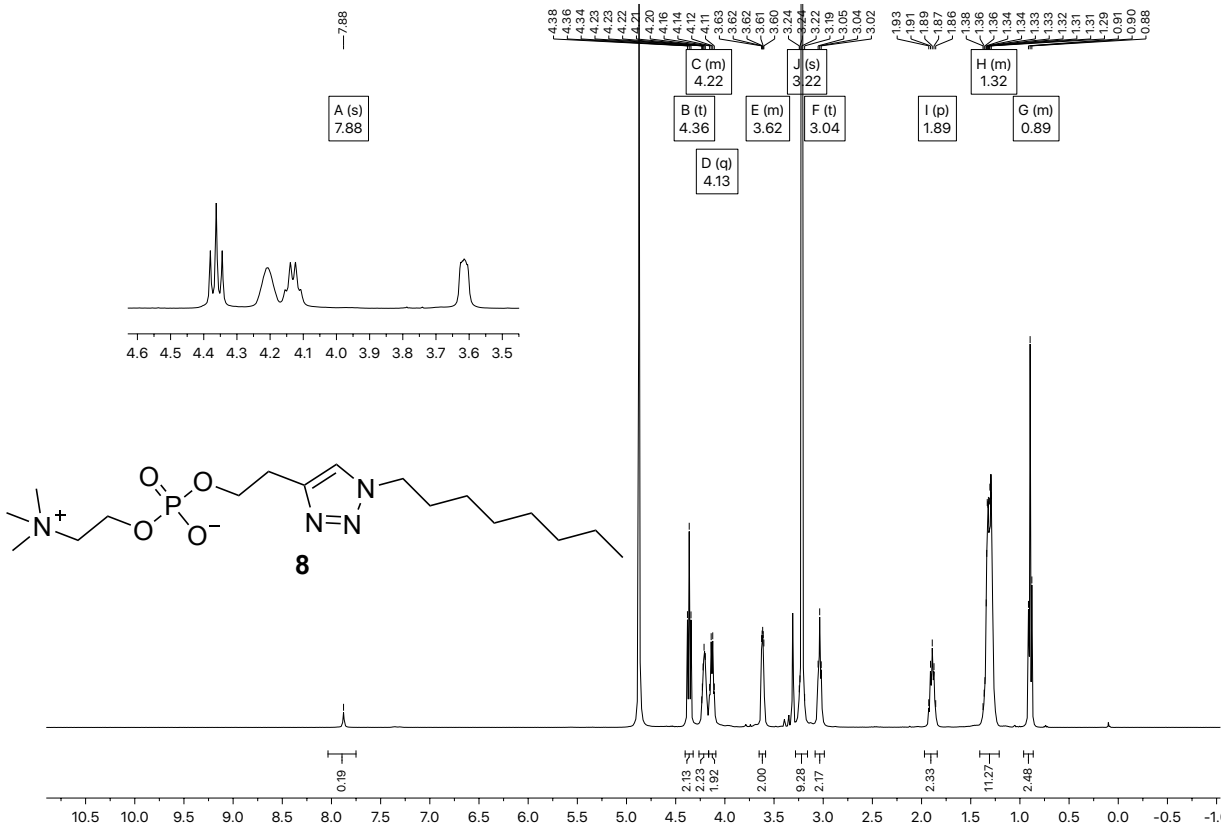

Figure S18: ^{1}H NMR spectrum of **8** in CD_3OD.

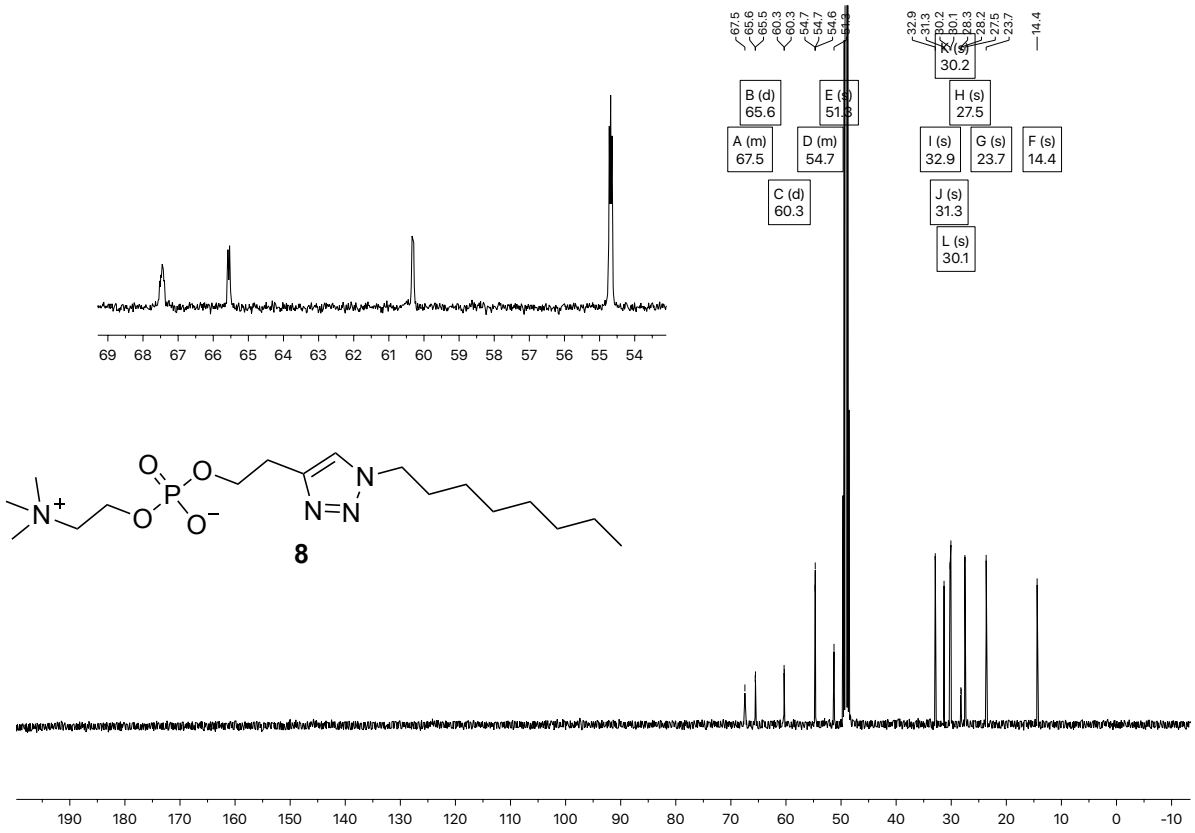

Figure S19: ^{13}C NMR spectrum of **8** in CD_3OD.

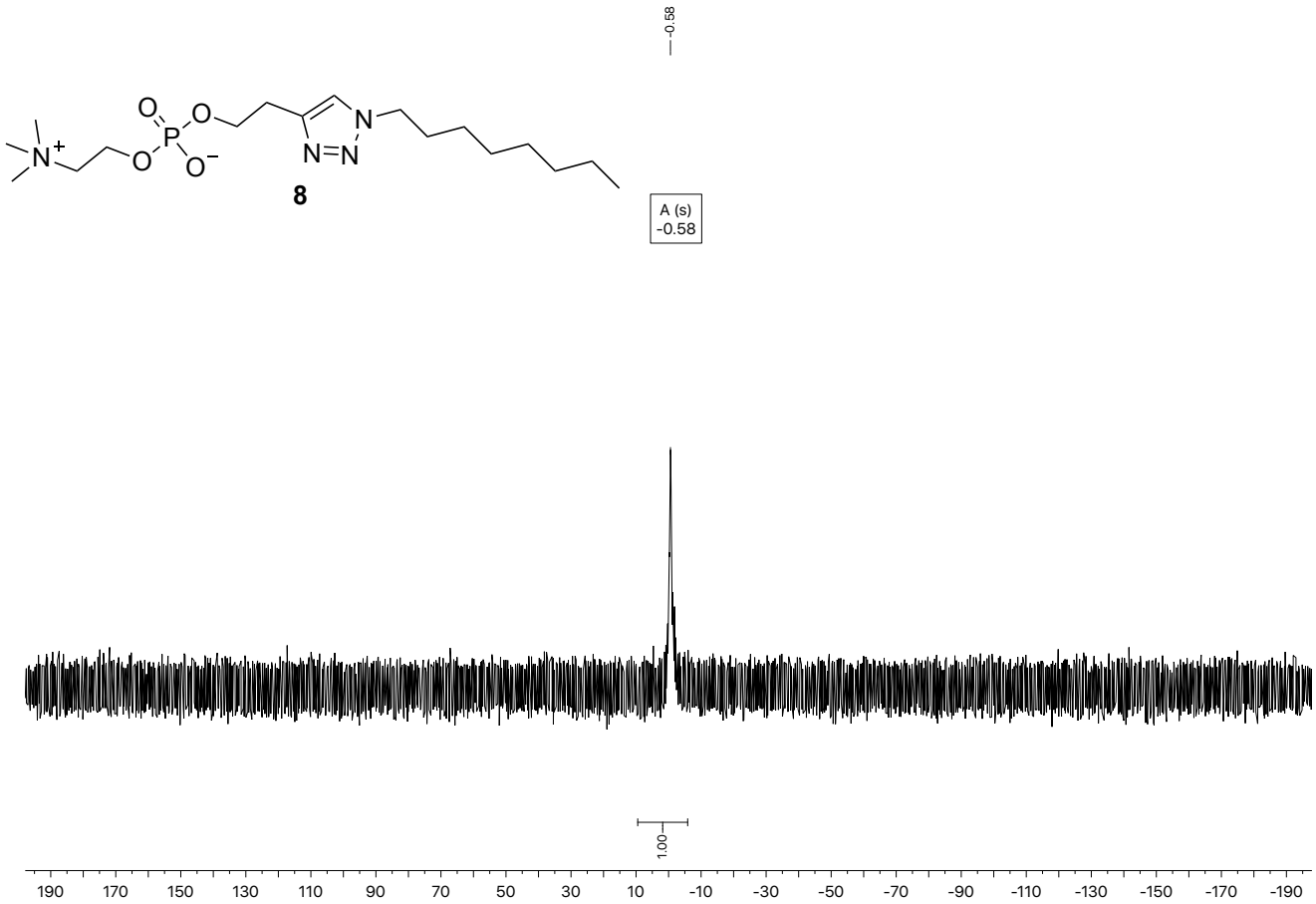

Figure S20: ^{31}P NMR spectrum of **8** in CD_3OD.

DOSY Data

Entry	Species present	*D* (3)	*D* (2)	*D* (ligand)	*D* (1)	*D* (TMS)
N	**A** (saturated)	-	-	9.1	-	7.0
O	[Cu-**A**)] (6.8 mM)	-	-	5.8	-	13
P	**3** (2 mM) + [Cu-**A**)] (6.8 mM)	3.7	-	5.7	-	8.0
Q	**3** (22 mM) + [Cu-**A**] (6.8 mM)	1.3	-	5.7	-	1.6
R	**3** (2 mM) + **B** (8.3 mM)	3.7	-	4.1	-	-
S	**3** (22 mM) + **B** (8.3 mM)	1.3	-	3.9	-	1.3
T	[Cu-**B**] (8.3 mM) + **2** (Saturated)	-	19	2.3	-	-
U	**3** (22 mM) + **C** (Saturated)	1.3	-	1.0	-	1.5

Table S1: Diffusion coefficients extracted from DOSY experiments. The diffusion coefficients were recorded for all reaction components at the concentrations present in the system during the synthesis of **3** in water. *D* values reported in 10^{-10} m^2s^{-1}. This table is an extension of the Table 1 in the main paper. The Morris' correlation[1] for small molecules predicts a MW of 516 g/mol for entry **A**, a MW of 379.3 g/mol for entry **I**, a MW of 339.5 g/mol for entry **E**. These predicted values are in close agreement with the actual molecular weights considering the model used for the predictions.

Inverted system

Entry	Species present	*D* (6)	*D* (5)	*D* (ligand)	*D* (4)	*D* (TMS)
L	**6** (60 mM) + **5** (saturated)	1.4	0.82	-	-	-
M	**6** (3 mM) + **B** (8.3 mM)	3.3	-	3.7	-	7.2
N	**6** (30 mM) + **B** (8.3 mM)	2.2	-	3.5	-	2.1
O	**6** (30 mM) + **C** (Saturated)	2.2	-	1.5	-	2.1
P	**4** (91 mM) + [Cu-**B**] (8.3 mM)	-	-	2.2	3.6	-
Q	**6** (30 mM) + **4** (91 mM) + [Cu+**B**] (8.3 mM)	1.7	-	2.4	3.0	-

Table S2: Diffusion coefficients extracted from DOSY experiments. The diffusion coefficients were recorded for all reaction components at the concentrations present in the system during the synthesis of **6** in water. *D* values reported in 10^{-10} m^2s^{-1}. This table is an extension of the Table 2 in the main paper.

NOTE:
Entry **P** might indicate association of the alkyne and with the copper-ligand **B** complex.
Entry **Q** shows slower diffusion of alkyne **4** in the presence of both copper-ligand **B** complex and surfactant **6**. This could indicate that when all three components are present association between surfactant and alkyne occurs however because of large overlap of the signals it is hard to say with certainty that these diffusion coefficients are correct.

Fluorimetry Data

The critical micelle concentrations of the surfactants was determined with a fluorimetric procedure reported by London *et al*.[2] The fluorescent molecule 1,6-diphenyl-1,3,5-hexatriene (DPH) emits a large increase in fluorescence when present in an apolar environment such as the micellar interior when a surfactant exceeds the critical micelle concentration. This property was used to determine the unknown CMC of various surfactant compounds. Fluorescence measurements were made with an Edinburgh Instruments Spectrofluorometer FS5 model. Instrument control and data processing were performed using Fluoracle software. The excitation wavelength was 358 nm and the emission wavelength was 430 nm. The excitation and emission slits were set at bandwidths of 1 nm. In all experiments, 1 cm path length quartz cuvettes were used. The protocol for CMC determination was as follows: 3 μL of 5 mM DPH dissolved in THF was added to various amounts of surfactant dissolved in a total volume of 3 ml of aqueous solution. The intercept of two trendlines, through the data points before and after the spike in fluorescence, was taken as the CMC.

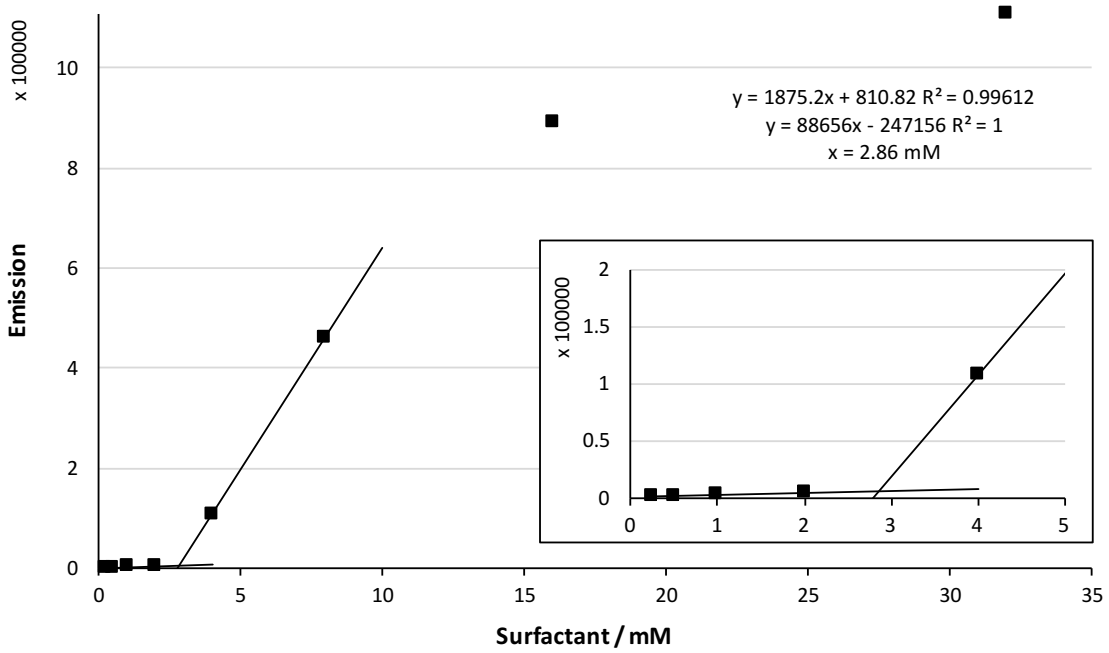

Figure S21: a CMC of 2.86 mM was extracted from a plot of fluorescence measurements at various concentration for surfactant **3**.

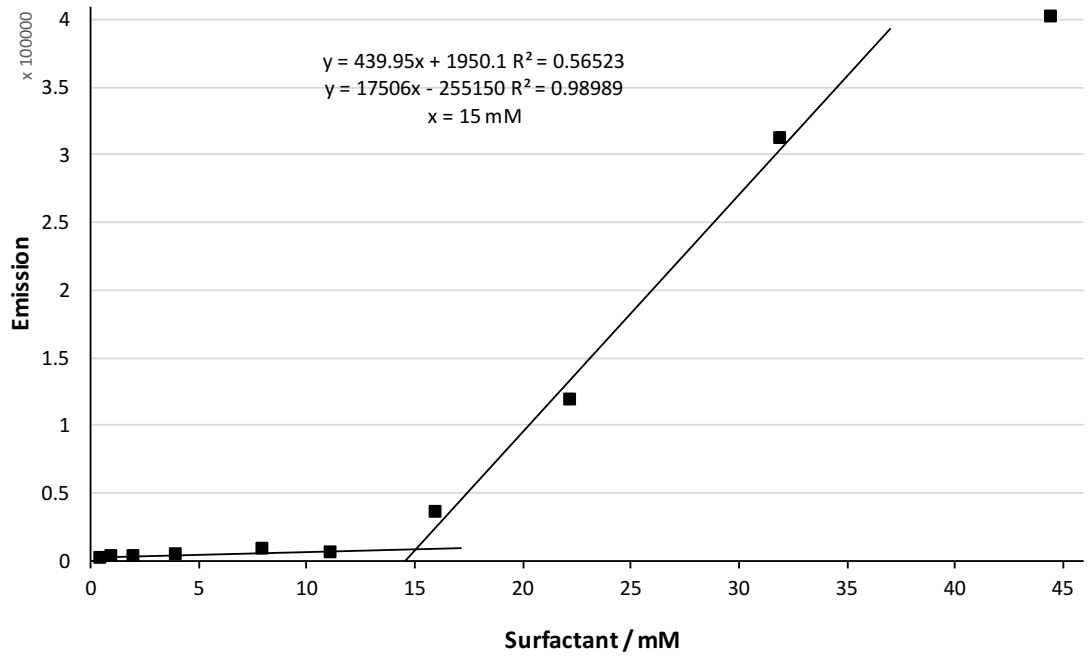

Figure S22: a CMC of 15 mM was extracted from a plot of fluorescence measurements at various concentration for surfactant **6**.

DLS data

Samples were prepared by dissolving an amount of surfactant in 1 mL of ultrapure Milli-Q water at a concentration above the CMC. This solution was filtered through a 0.2 µm PTFE filter right before performing a DLS measurement.

Sample Name:	EP_decyne_24mM 1		
SOP Name:	mansettings.nano		
File Name:	Sarah.dts	**Dispersant Name:**	Water
Record Number:	61	**Dispersant RI:**	1.330
Material RI:	1.59	**Viscosity (cP):**	0.8872
Material Absorbtion:	0.010	**Measurement Date and Time:**	19 December 2016 1:45 pm

Temperature (°C):	25.0			**Duration Used (s):**	60
Count Rate (kcps):	377.7			**Measurement Position (mm):**	3.00
Cell Description:	Disposable micro cuvette (40µl)			**Attenuator:**	11

			Size (d.nm):	**% Intensity:**	**St Dev (d.nm):**
Z-Average (d.nm):	6.983	**Peak 1:**	7.541	90.5	3.117
PdI:	0.260	**Peak 2:**	1543	9.5	960.0
Intercept:	0.730	**Peak 3:**	0.000	0.0	0.000
Result quality :	Good				

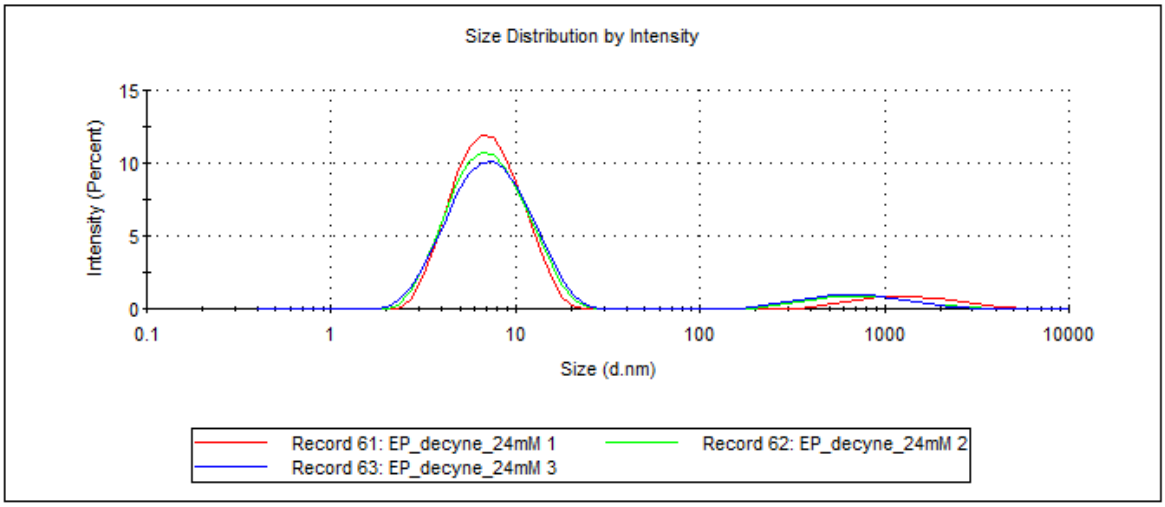

Figure S23: The size distribution by intensity of a DLS measurement of surfactant **3** at 24 mM indicates micelle aggregates with a size of around 7.5 nm.

Sample Name:	EP140flipfiltered 1		
SOP Name:	Water-25C.sop		
File Name:	210817.dts	**Dispersant Name:**	Water
Record Number:	4	**Dispersant RI:**	1.330
Material RI:	1.45	**Viscosity (cP):**	0.8872
Material Absorbtion:	0.001	**Measurement Date and Time:**	21 August 2017 2:04 pm

Temperature (°C):	25.0	**Duration Used (s):**	60
Count Rate (kcps):	330.6	**Measurement Position (mm):**	3.00
Cell Description:	Disposable micro cuvette (40µl)	**Attenuator:**	11

			Size (d.nm):	**% Intensity:**	**St Dev (d.nm):**
Z-Average (d.nm):	5.580	**Peak 1:**	5.938	91.0	2.604
PdI:	0.240	**Peak 2:**	845.9	9.0	609.8
Intercept:	0.730	**Peak 3:**	0.000	0.0	0.000

Result quality : Good

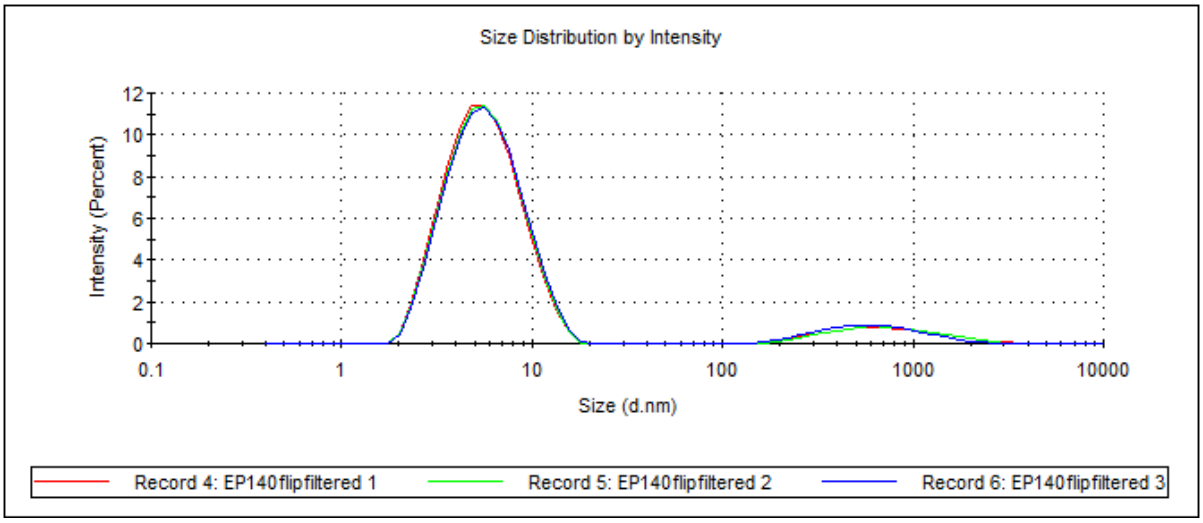

Figure S24: The size distribution by intensity of a DLS measurement of surfactant **6** at 30 mM indicates micelle aggregates with a size of around 6 nm.

Kinetic Data

^{1}H NMR spectra of key water soluble reaction components in D_2O

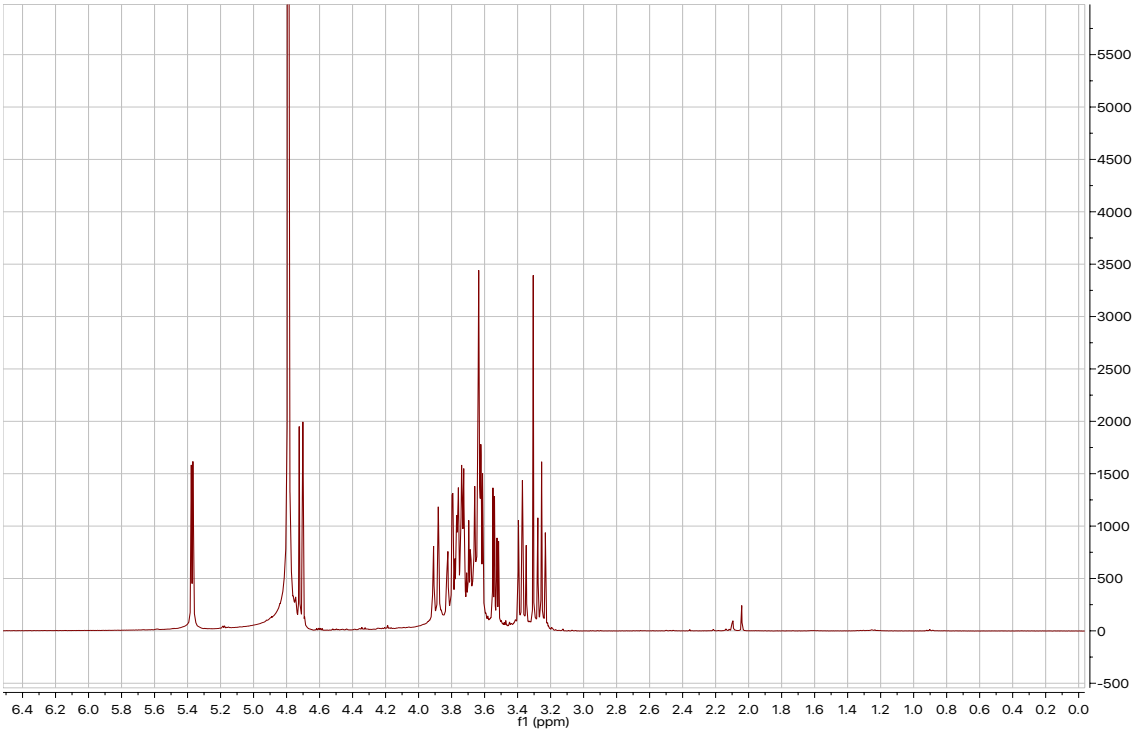

Figure S25: ^{1}H NMR spectrum of 1-deoxy-1-azido-β-D-maltopyranose **1** in D_2O.

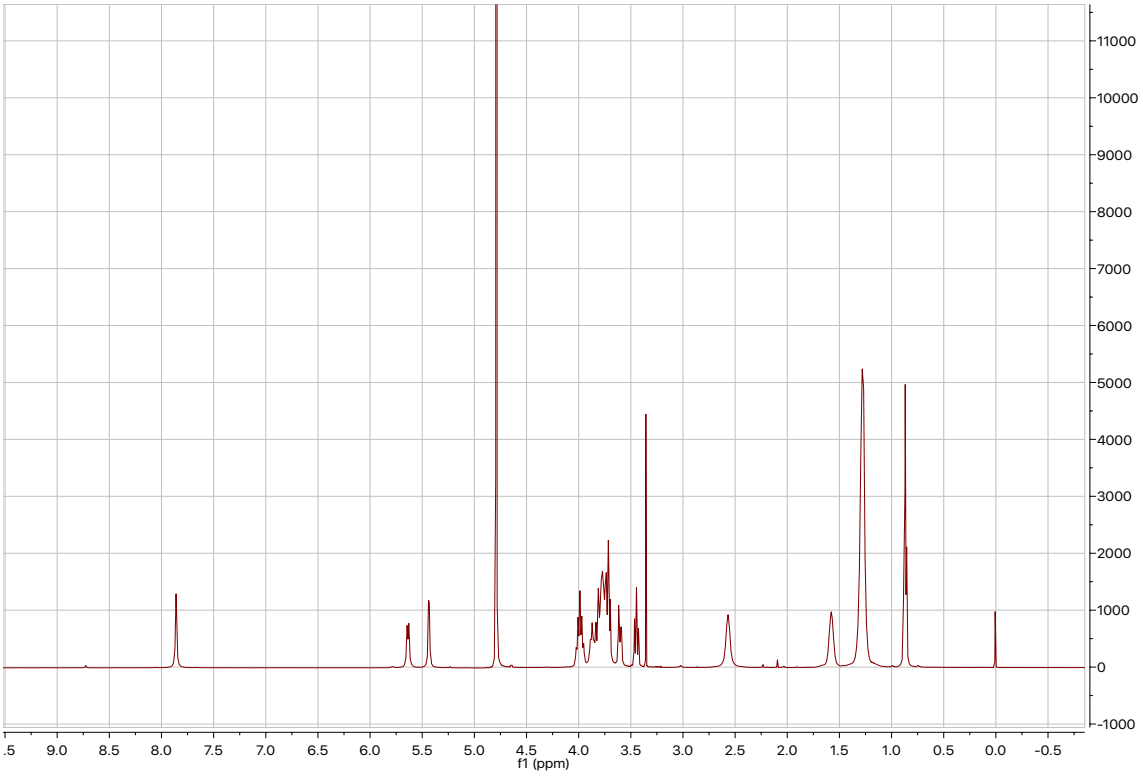

Figure S26: ^{1}H NMR spectrum of 1-(1-deoxy-β-D-maltopyranosyl)-4-octyl triazole **3** in D_2O.

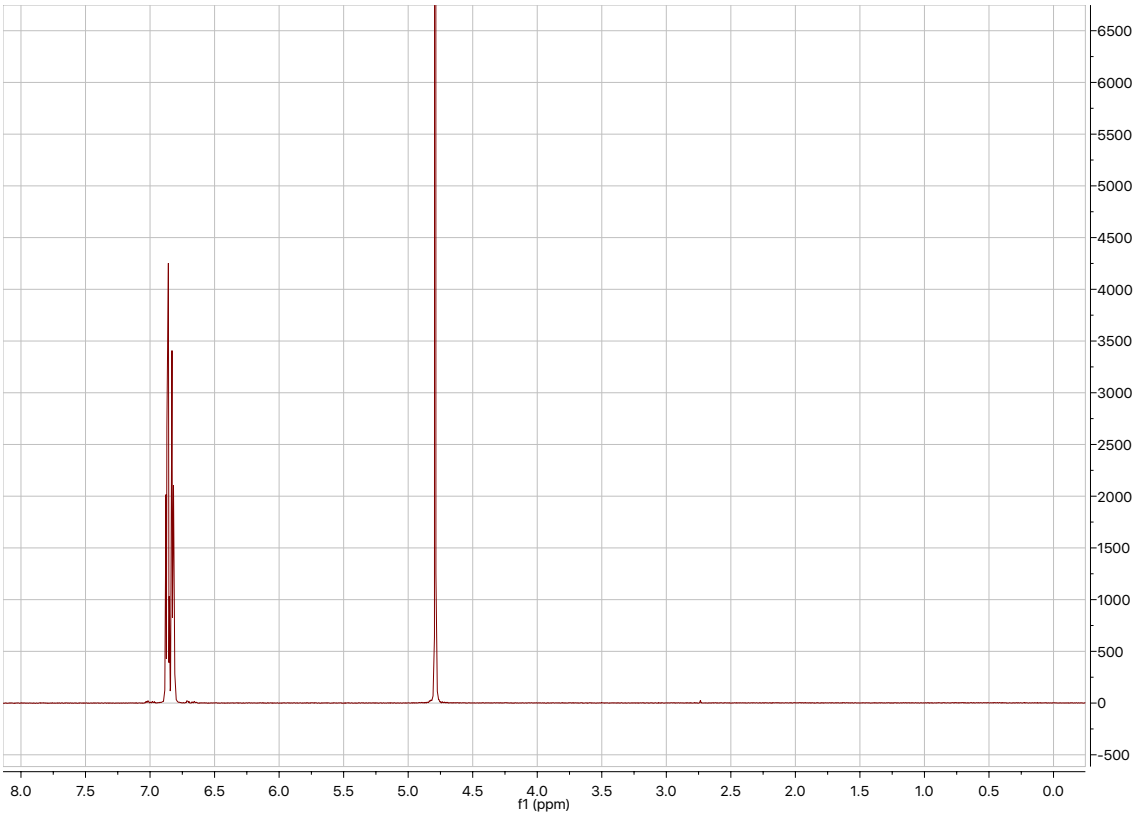

Figure S27: ^{1}H NMR spectrum of ligand **A** in D_2O.

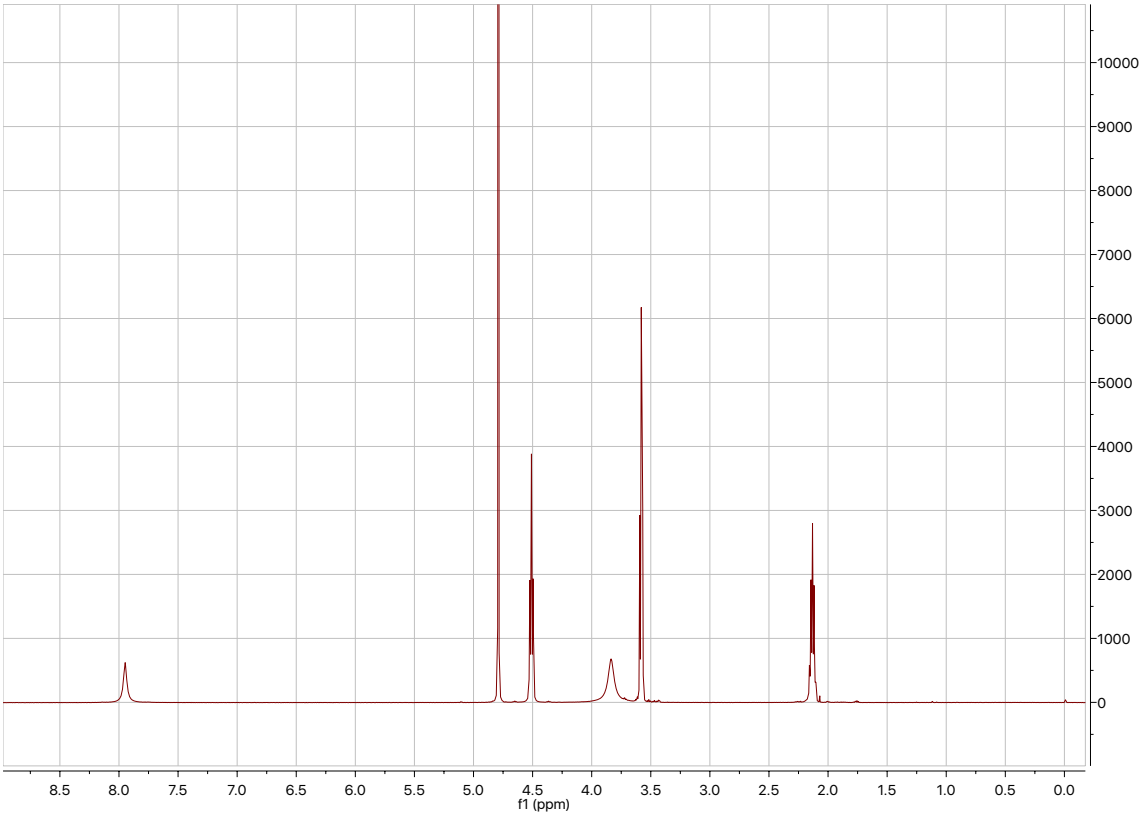

Figure S28: ^{1}H NMR spectrum of ligand **B** in D_2O.

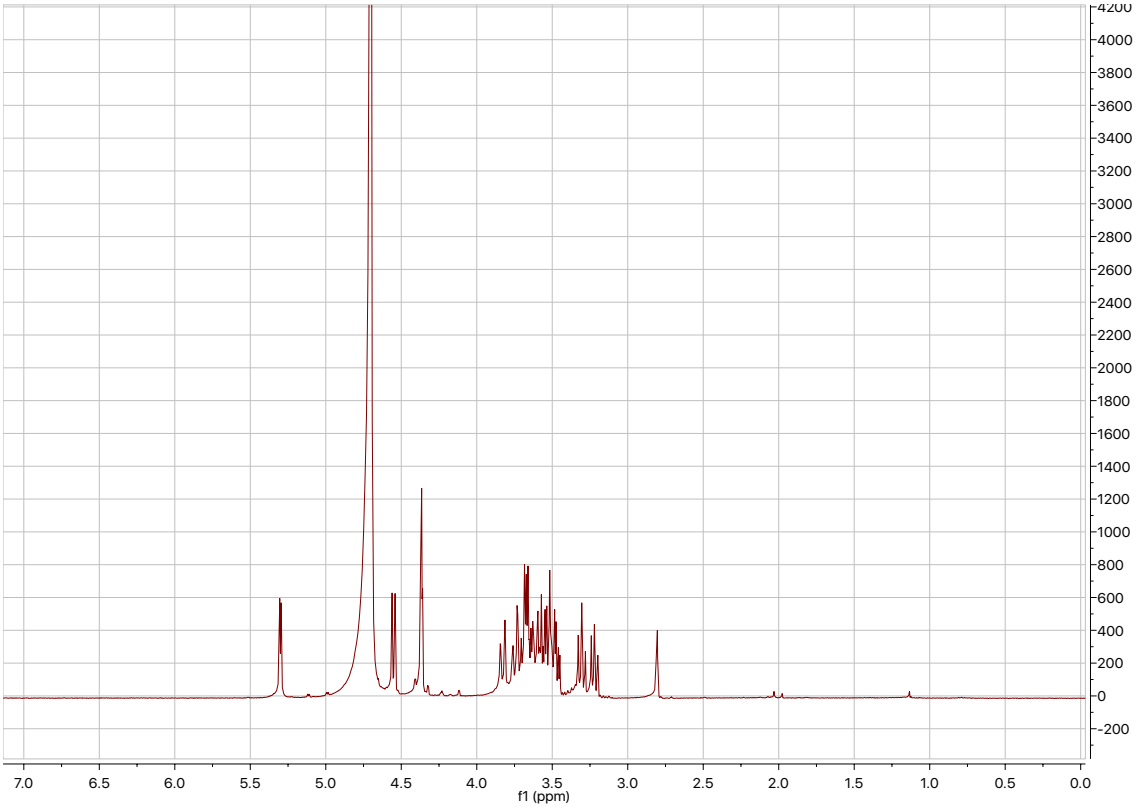

Figure S29: ^{1}H NMR spectrum of propargyl-β-D-maltopyranoside **4** in D_2O.

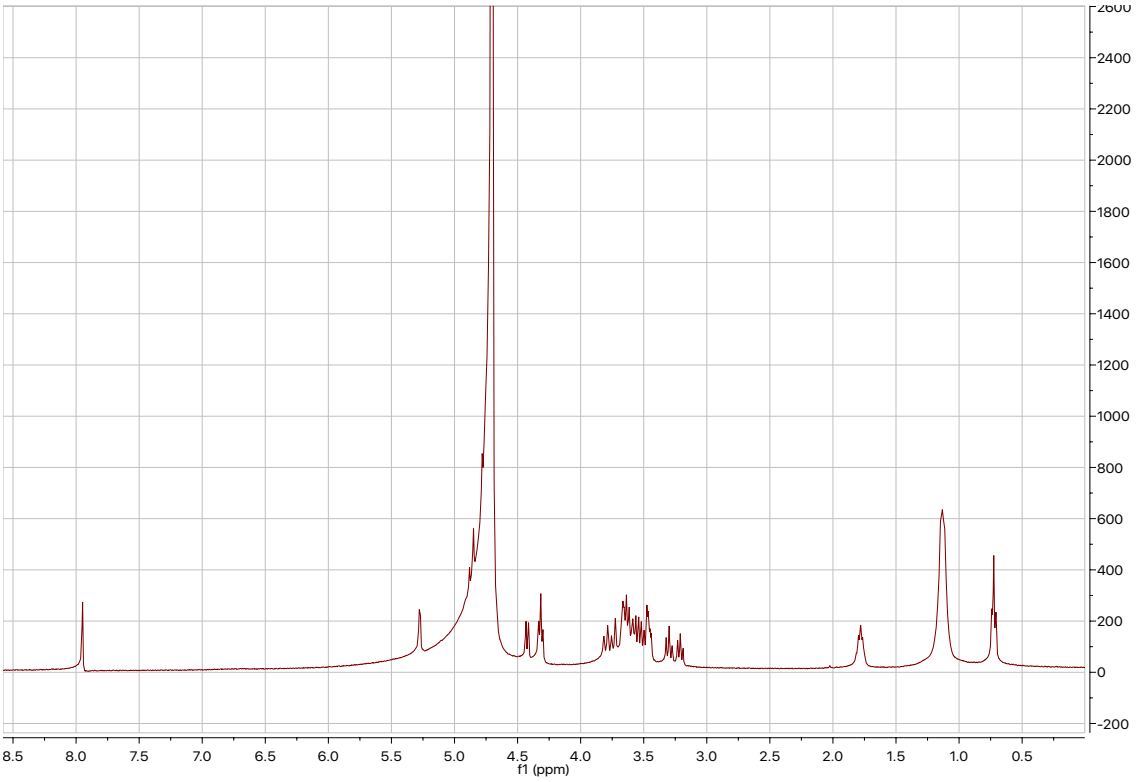

Figure S30: ^{1}H NMR spectrum of 1-octyl-4-(propargyl-β-D-maltopyranosidyl) triazole **6** in D_2O.

Stacked Spectra of Kinetic ^{1}H NMR Experiments

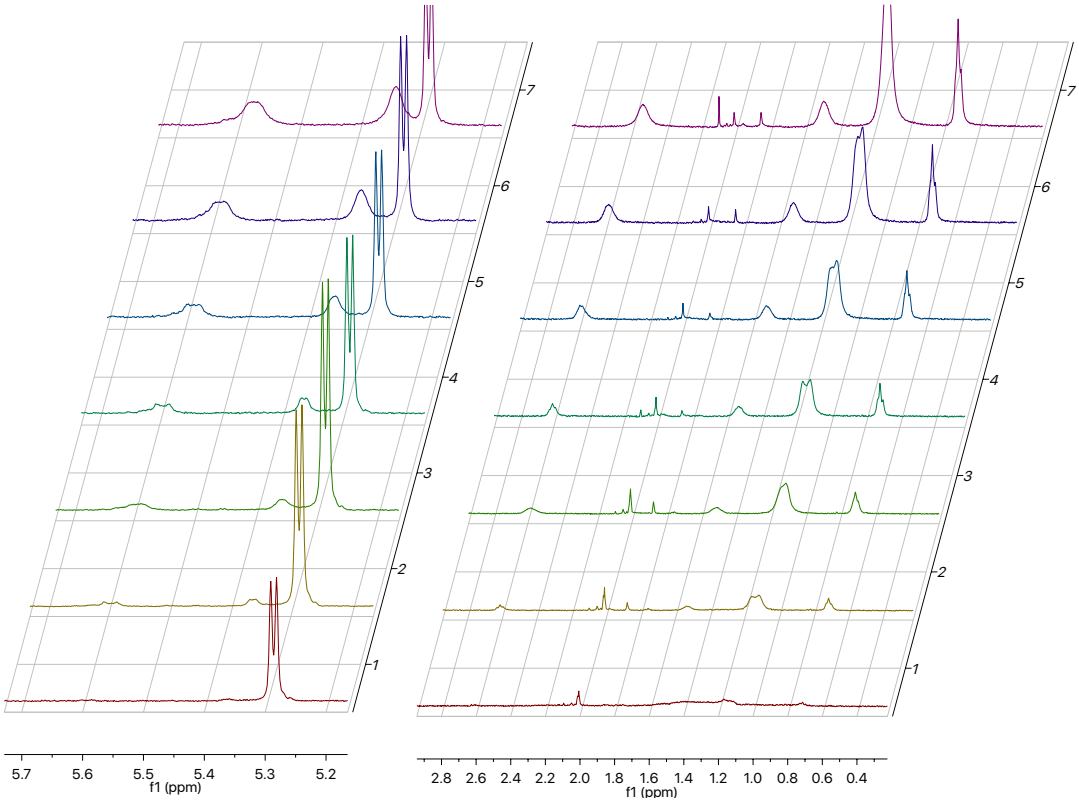

Figure S31: Stacked ^{1}H NMR spectra of the unseeded reaction of **1** with **2** and ligand **A**. Data plotted in Figure 2, B.

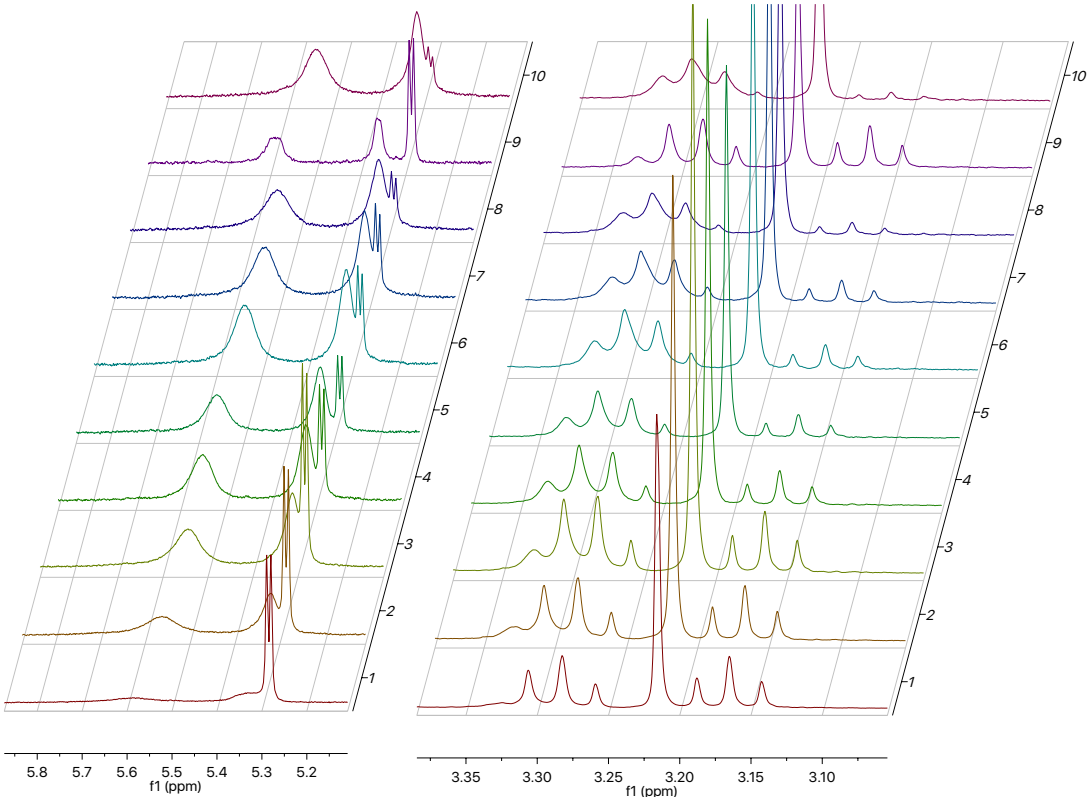

Figure S32: Stacked ^{1}H NMR spectra of the seeded reaction of **1** with **2** and ligand **A** seeded with **3**. Data plotted in Figure 2, C.

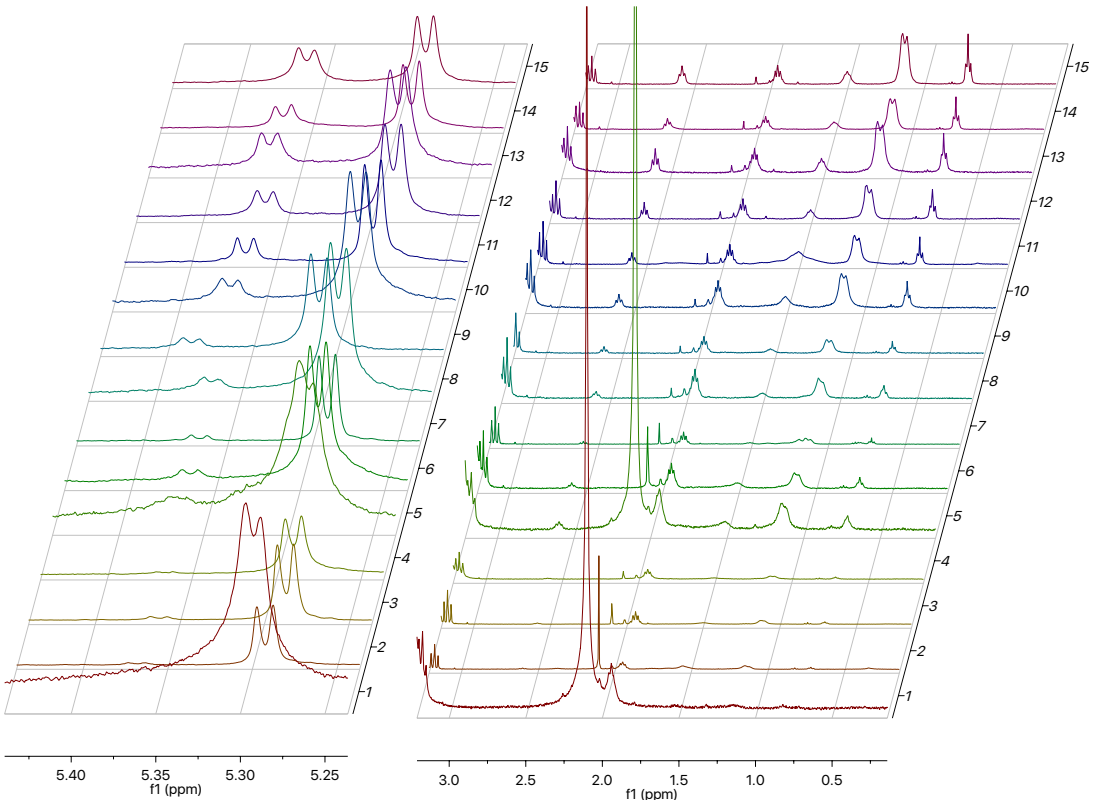

Figure S33: Stacked ^{1}H NMR spectra of the unseeded reaction of **1** with **2** and ligand **B**. Data plotted in Figure 2, B.

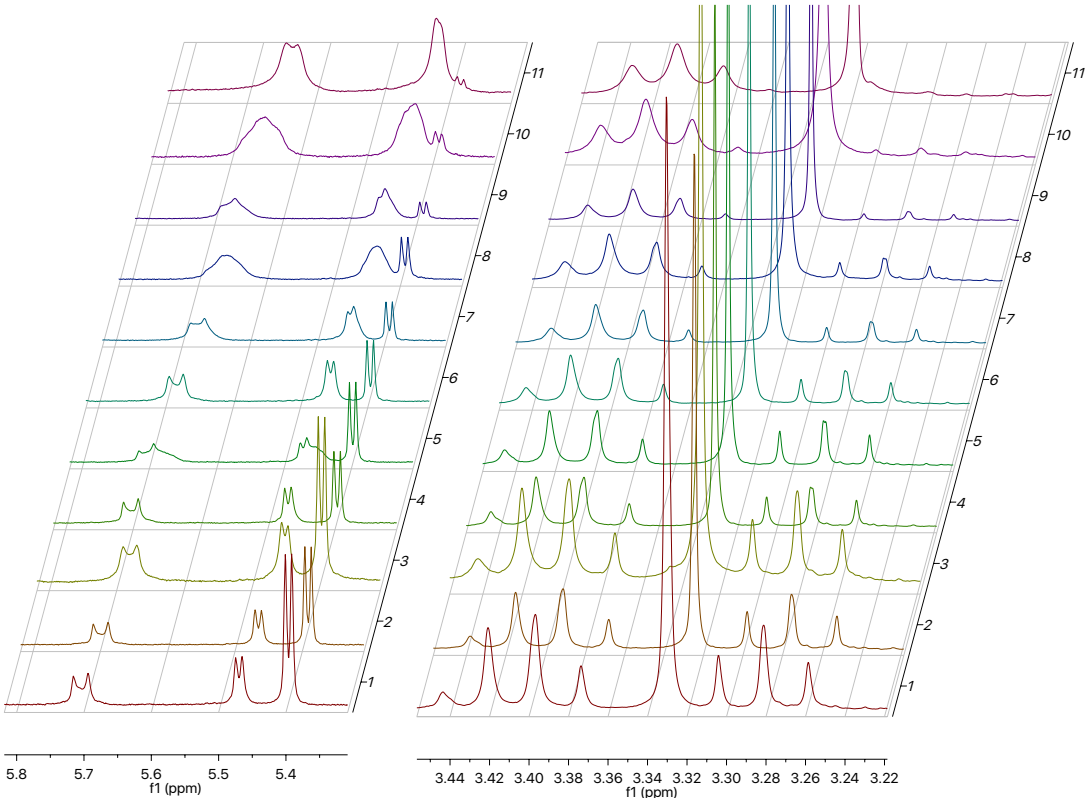

Figure S34: Stacked ^{1}H NMR spectra of the seeded reaction of **1** with **2** and ligand **B** seeded with **3**. Data plotted in Figure 2, C.

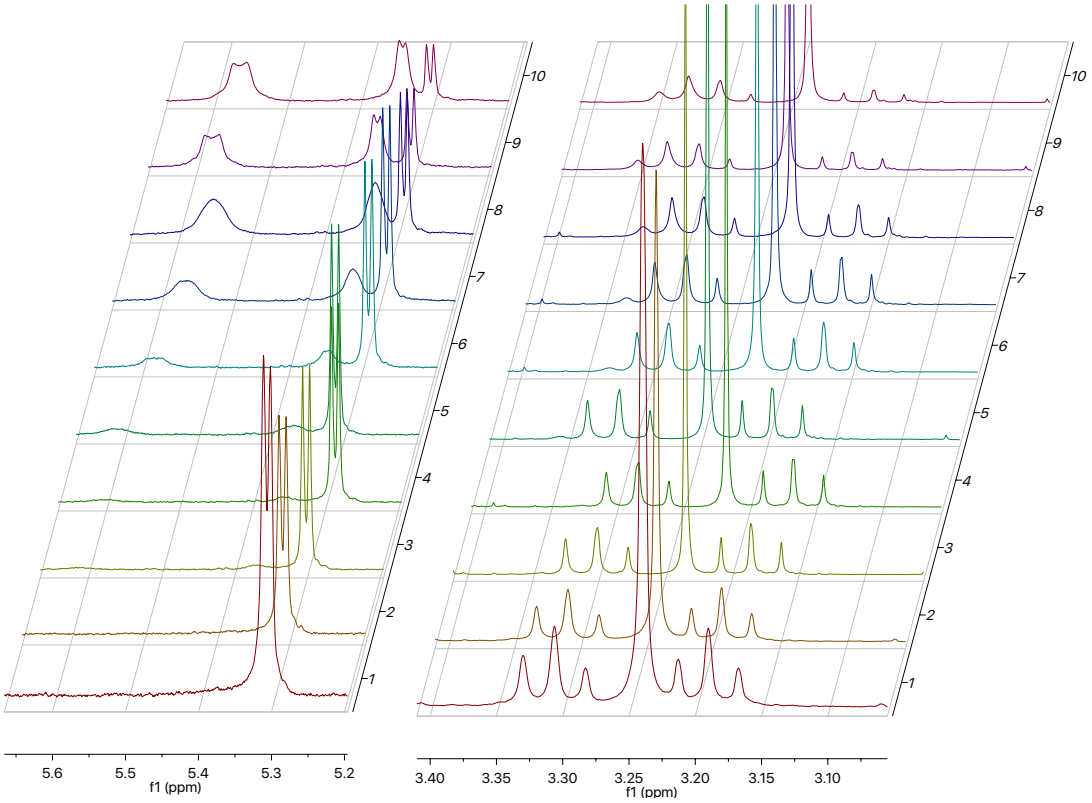

Figure S35: Stacked ^{1}H NMR spectra of the unseeded reaction of **1** with **2** and ligand **C**. Data plotted in Figure 2, B.

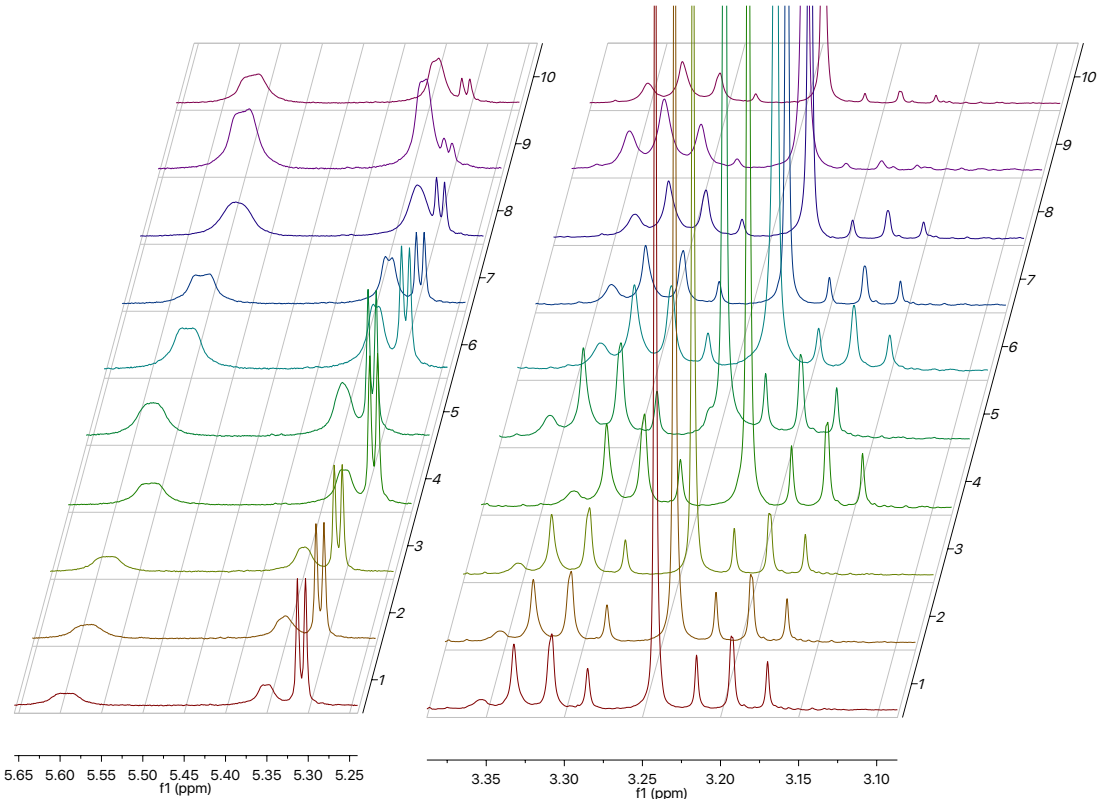

Figure S36: Stacked ^{1}H NMR spectra of the seeded reaction of **1** with **2** and ligand **C** seeded with **3**. Data plotted in Figure 2, C.

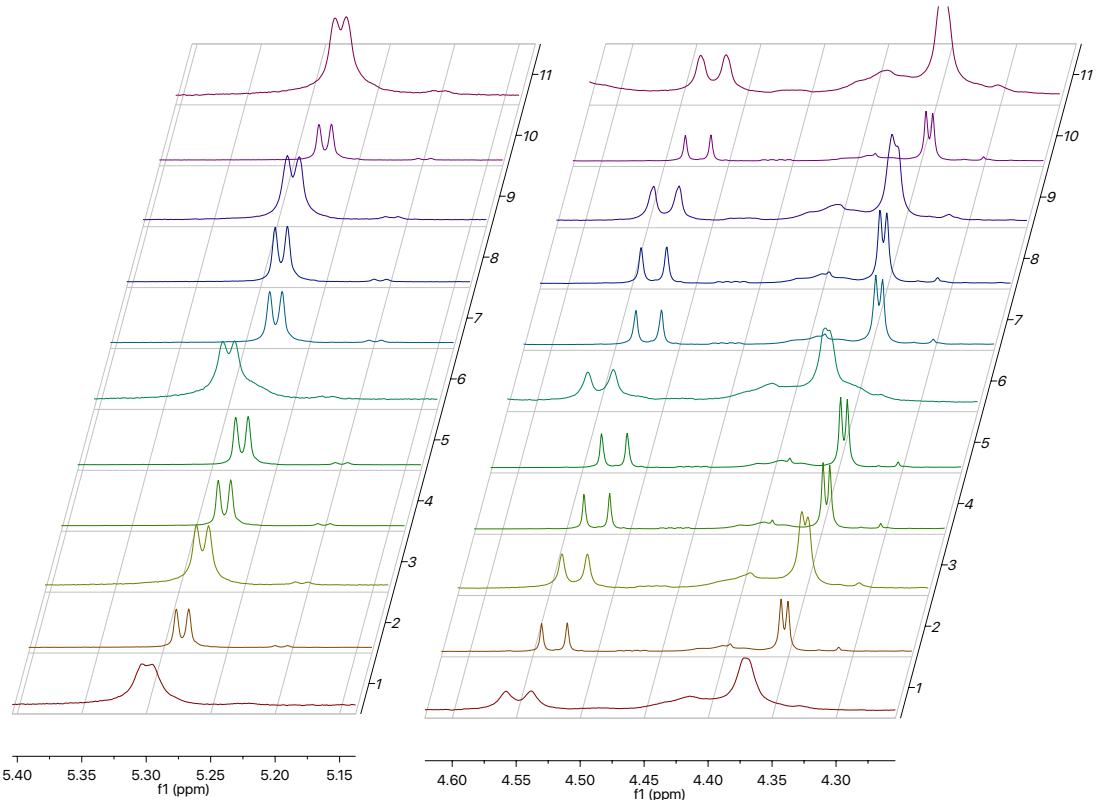

Figure S37: Stacked ^{1}H NMR spectra of the unseeded reaction of **4** with **5** and ligand **B**. Data plotted in Figure 5, B.

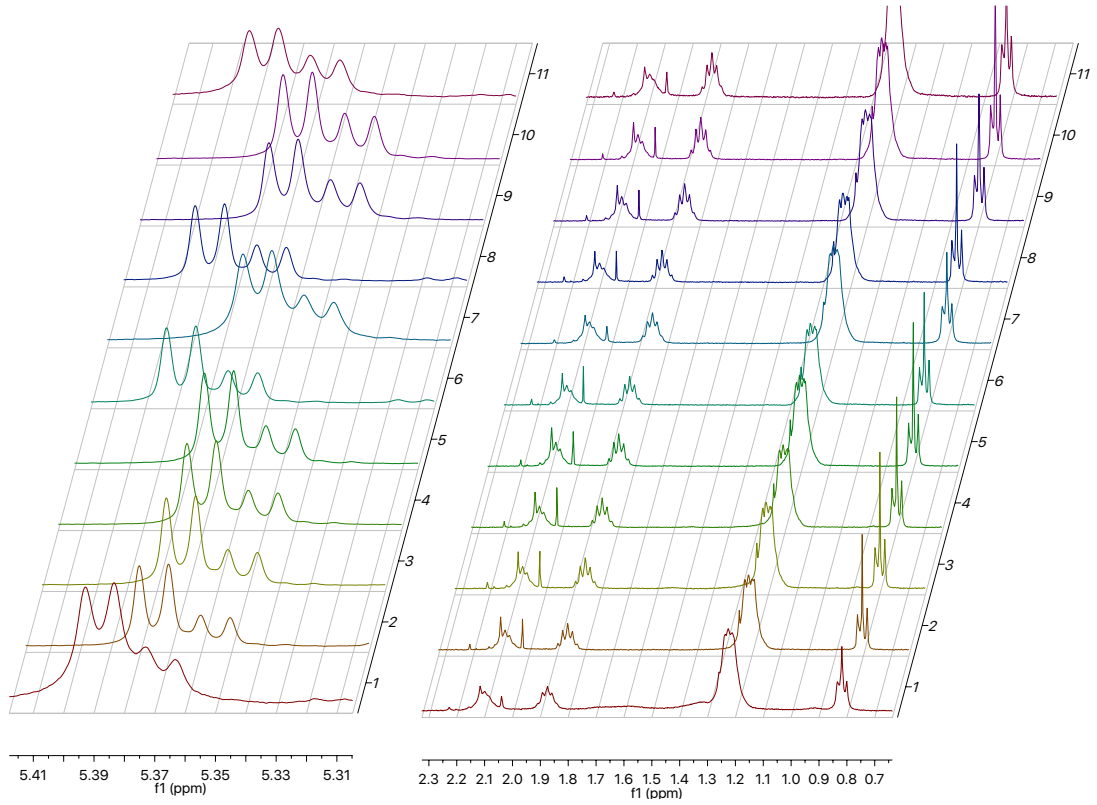

Figure S38: Stacked ^{1}H NMR spectra of the seeded reaction of **4** with **5** and ligand **B** seeded with **6**. Data plotted in Figure 5, C.

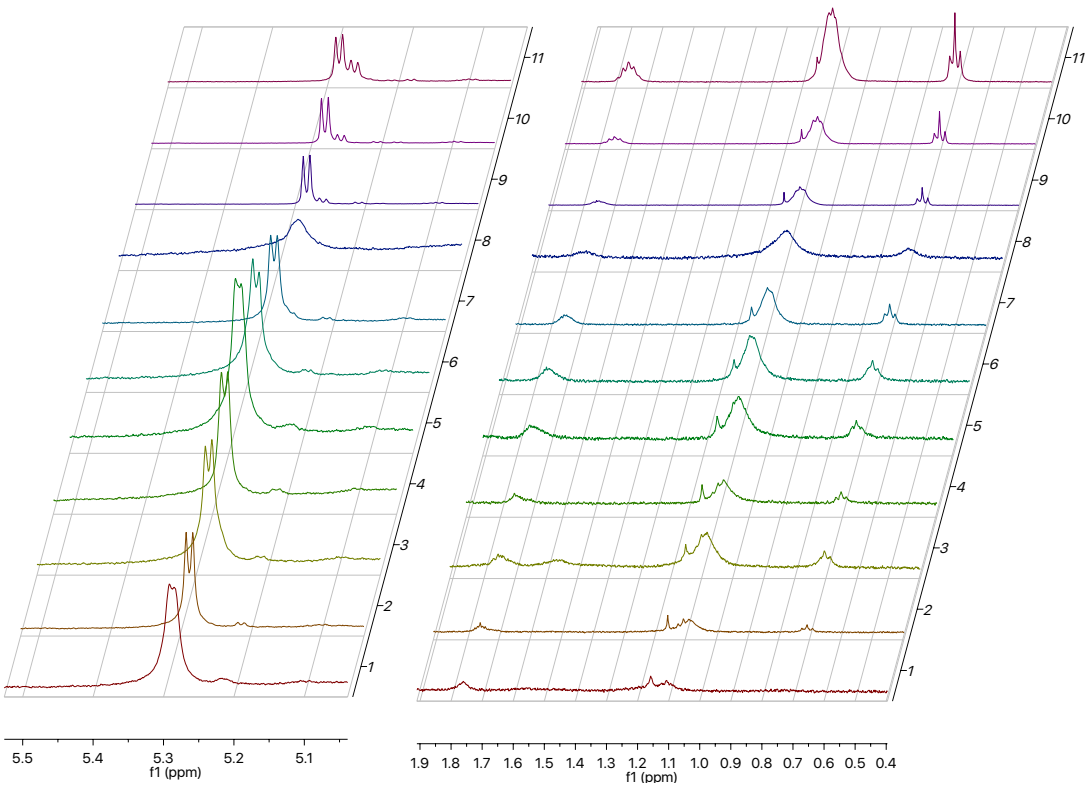

Figure S39: Stacked ^{1}H NMR spectra of the unseeded reaction of **4** with **5** and ligand **C**. Data plotted in Figure 5, B.

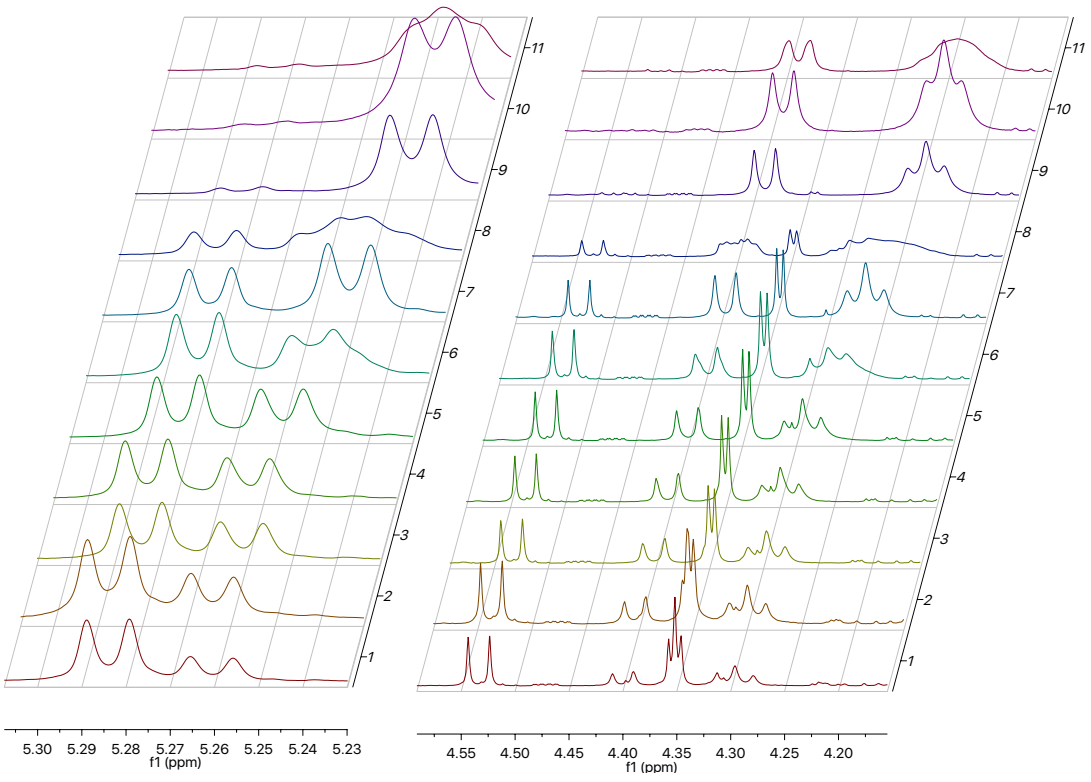

Figure S40: Stacked ^{1}H NMR spectra of the seeded reaction of **4** with **5** and ligand **C** seeded with **6**. Data plotted in Figure 5, C.

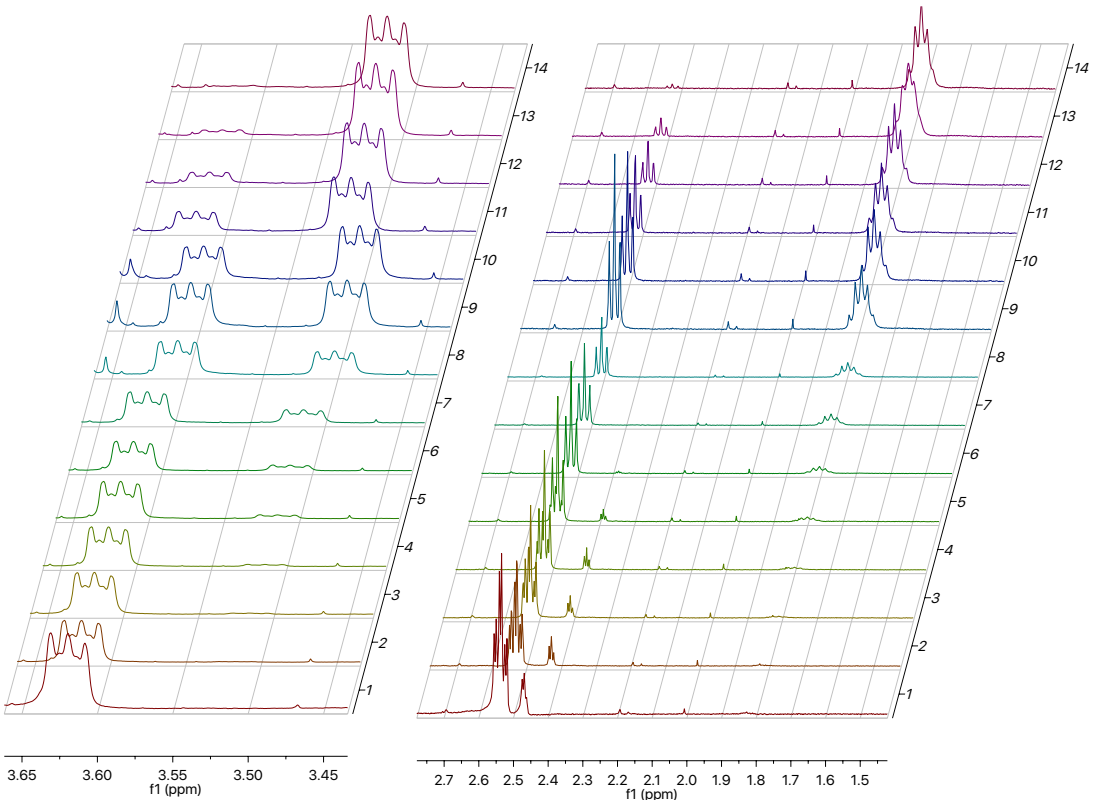

Figure S41: Stacked ^{1}H NMR spectra of the unseeded reaction of **7** with **5** and ligand **C**. Data plotted in Figure 8, B.

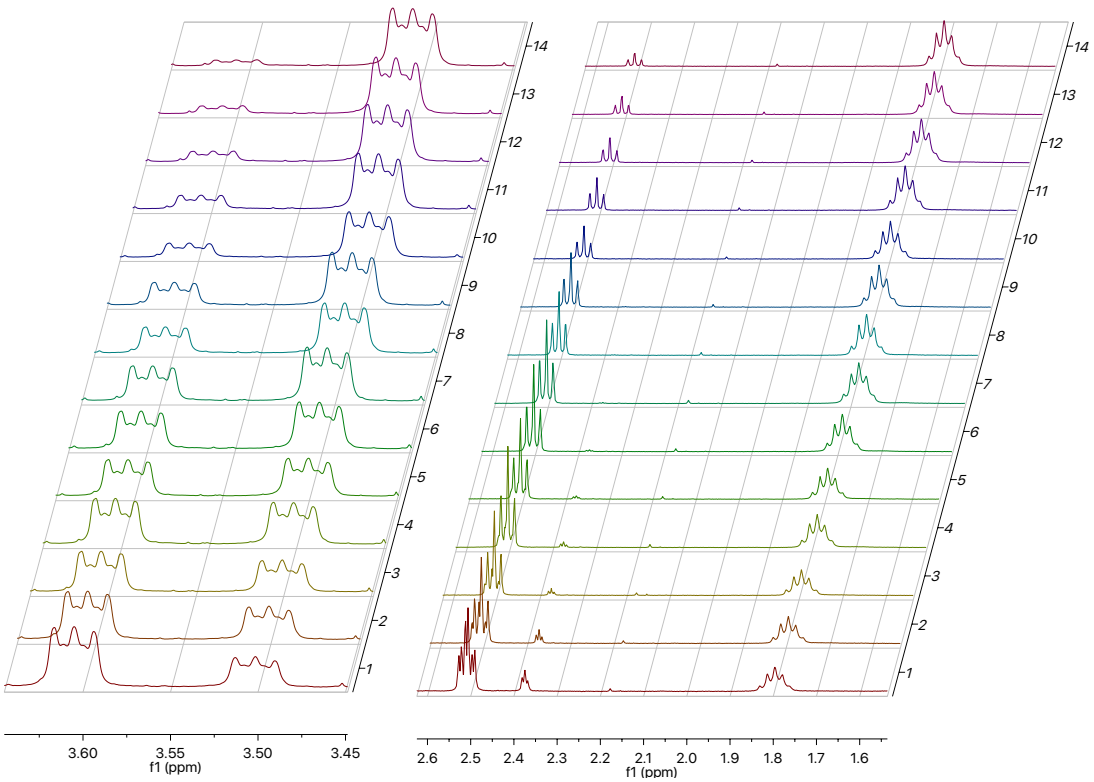

Figure S42: Stacked ^{1}H NMR spectra of the unseeded reaction of **7** with **5** and ligand **C** seeded with **6**. Data plotted in Figure 8, B.

Tables of extracted reaction rates

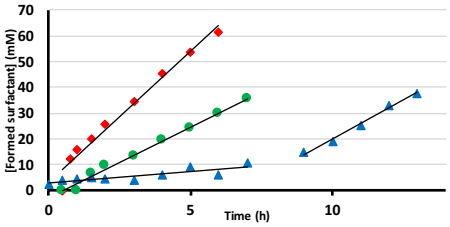

Ligand A	Ligand B_1	Ligand B_2	Ligand C
V_{max} = 5.86 ± 0.13 mM h^{-1}	V_{lag} = 0.922 ± 0.06 mM h^{-1}	V_{max} = 5.72 ± 0.34 mM h^{-1}	V_{max} = 10.2 ± 1.80 mM h^{-1}
R^2 = 0.988	R^2 = 0.747	R^2 = 0.992	R^2 = 0.972

Table S3: Maximum rate of conversion with standard deviation over three independent repeats extracted from Figure 2, **B** with a trend line. Where B_1 is from data points during the lag period and B_2 is after the lag period.

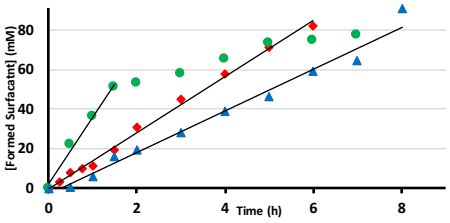

Ligand A	Ligand B	Ligand C
V_{max} = 33.5 ± 2.00 mM h^{-1}	V_{max} = 10.7 ± 0.01 mM h^{-1}	V_{max} = 14.1 ± 1.69 mM h^{-1}
R^2 = 0.989	R^2 = 0.997	R^2 = 0.996

Table S4: Maximum rate of conversion with standard deviation over three independent repeats extracted from Figure 2, **C** with a trendline.

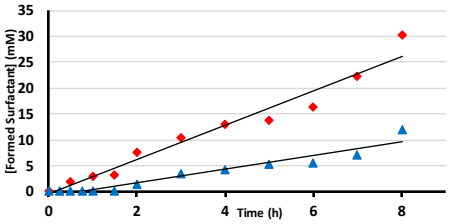

Ligand B	Ligand C
V_{lag} = 1.46 ± 0.60 mM h^{-1}	V_{max} = 3.35 ± 0.97 mM h^{-1}
R^2 = 0.806	R^2 = 0.957

Table S5: Maximum rate of conversion with standard deviation over three independent repeats extracted from Figure 5, **B** with a trendline.

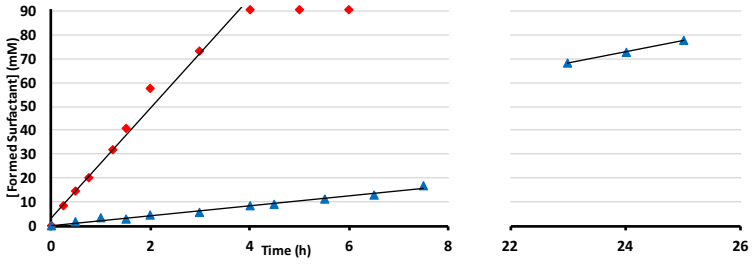

Ligand B_1	Ligand B_2	Ligand C
V_{lag} = 2.05 ± 0.28 mM h^{-1}	V_{max} = 4.64 ± 0.25 mM h^{-1}	V_{max} = 23.0 ± 0.63 mM h^{-1}
R^2 = 0.987	R^2 = 1	R^2 = 0.986

Table S6: Maximum rate of conversion with standard deviation over three independent repeats extracted from Figure 5, **C** with a trendline, where B_1 is from data points during the lag period and B_2 is after the lag period.

Control experiments

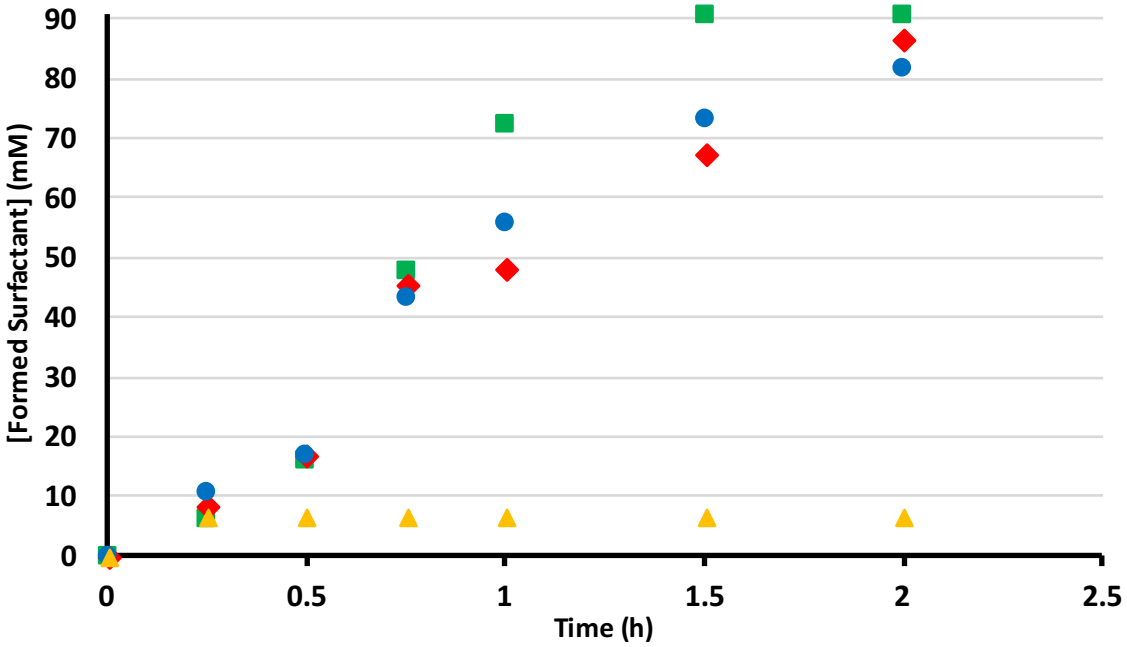

Figure S43: Reaction kinetics for CuAAC of three different ligands in tBuOH/D_2O (1:1) shows similar reaction rates for all ligands in a reaction between **1** and **2** to form **3**. Complete conversion in 2 hours and no lag period is observed for ligand **A** (green squares), ligand **B** (blue circles and ligand **C** (red diamonds). Catalyst deactivation occurs in the absence of ligand (yellow triangles).

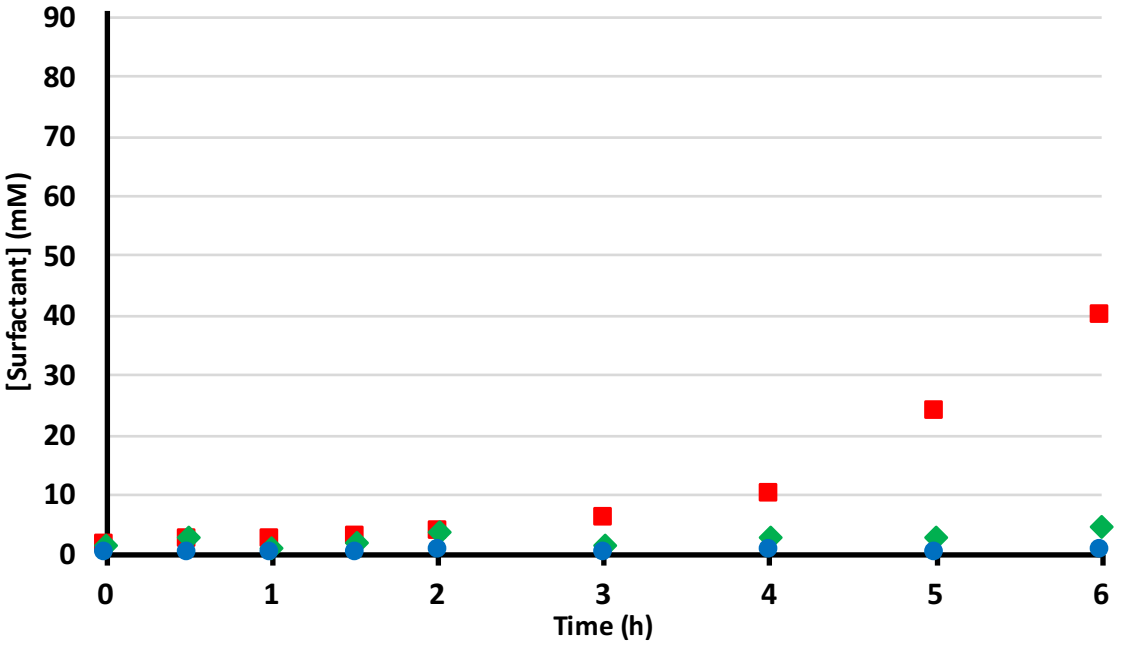

Figure S44: Control experiment investigating the influence of varying amounts ligand **B** on the lag period in the original system (CuAAC of maltose azide **1** with **2**). A rate increase is observed when using one equivalent (red squares) as opposed to the original 2 equivalents (green diamonds). When further increasing the amounts of ligand **B** to four equivalents (blue circles) no product formation is observed at all in the first 6 hours. Increasing the amount of ligand added therefor increases the duration of the lag period.

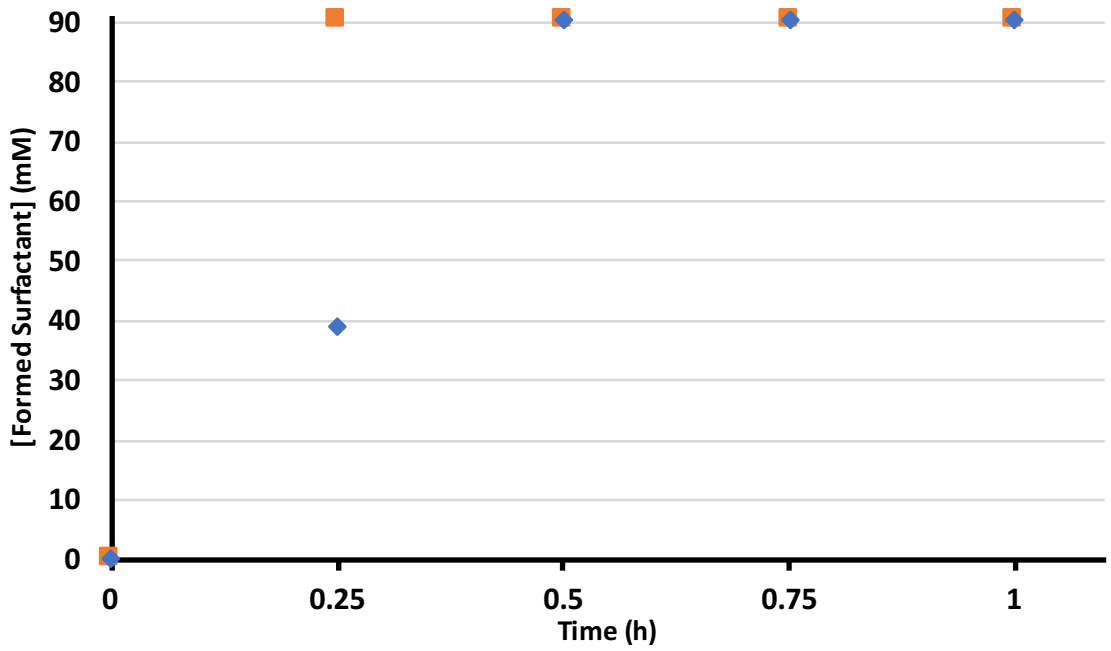

Figure S45: Reaction kinetics for CuAAC between **4** and **5** to form **6** with ligand **B** (blue diamonds) and ligand **C** (orange squares) in tBuOH/D_2O (1:1). Complete conversion in 30 minutes and no lag period are observed for both ligands.

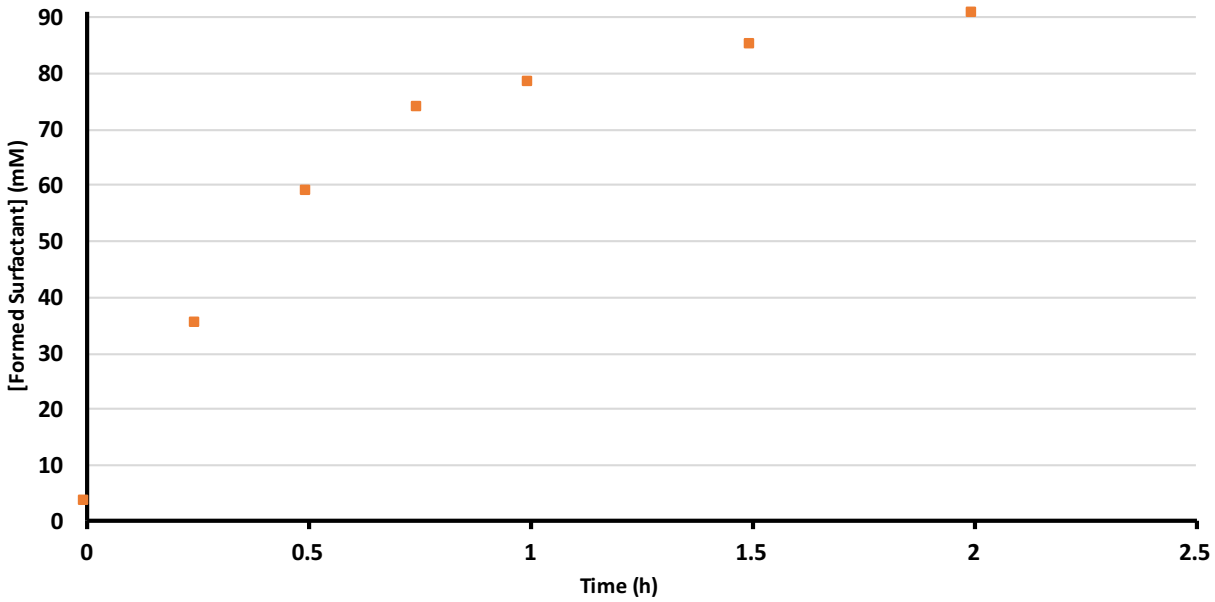

Figure S46: Reaction kinetics for CuAAC between **7** and **5** to form **8** with ligand **B** in tBuOH/D_2O (1:1). Complete conversion in 2 hours and no lag period are observed. A faster initial rate is observed compared to the original system described in figure S43.

References

(1) Evans, R.; Deng, Z.; Rogerson, A. K.; McLachlan, A. S.; Richards, J. J.; Nilsson, M.; Morris, G. A. Quantitative Interpretation of Diffusion-Ordered NMR Spectra: Can We Rationalize Small Molecule Diffusion Coefficients? *Angew. Chemie - Int. Ed.* **2013**, *52* (11), 3199–3202.

(2) Chattopadhyay, A.; London, E. Fluorimetric Determination of Critical Micelle Concentration Avoiding Interference from Detergent Charge. *Anal. Biochem.* **1984**, *139* (2), 408–412.